Shell oxygen isotope values and sclerochronology of the limpet *Patella vulgata* Linnaeus 1758 from northern Iberia: implications for the reconstruction of past seawater temperatures

Igor Gutiérrez-Zugasti[a], Roberto Suárez-Revilla[a], Leon J. Clarke[b], Bernd R. Schöne[c], Geoffrey N. Bailey[d], M. R. González-Morales[a]

[a] Instituto Internacional de Investigaciones Prehistóricas de Cantabria, Universidad de Cantabria. Edificio Interfacultativo, Avda. Los Castros s/n. 39005 Santander, Spain igorgutierrez.zug@gmail.com

[b]School of Science and the Environment, Faculty of Science and Engineering, Manchester Metropolitan University, Manchester, M1 5GD, UK

[c]Institute of Geosciences, University of Mainz, Johann-Joachim-Becherweg 21, 55128 Mainz, Germany

[d]Department of Archaeology, University of York, King's Manor YO1 7EP, York, UK

Abstract

Understanding environmental conditions faced by hunter-fisher-gatherers during the Pleistocene and Holocene, and interpretation of subsistence strategies, social organisation and settlement patterns, are key topics for the study of past human societies. In this respect, oxygen isotope values ($\delta^{18}O$) of mollusc shell calcium carbonate can provide important information on palaeoclimate and the seasonality of shell collection at archaeological sites. In this paper, we tested *P. vulgata* shells from northern Iberia as a paleoclimate archive through the study of shell oxygen isotope values and sclerochronology of modern samples. Results showed that limpets formed their shells close to isotopic equilibrium, with an average offset between measured and predicted values of 0.36 ‰. This offset is significantly reduced with respect to those reported in previous studies, probably due to the use of highly resolved data on the

isotopic composition of the water when calculating predicted values. Despite large intra-specific variability, shell growth patterns of *P. vulgata* revealed a common pattern of higher growth in spring and a growth cessation/slowdown in summer and winter. The seasonal growth cessation/slowdown did not exceed three months. Therefore, a correct interpretation of the season of shell collection is still possible. Reconstructed seawater temperature exhibited a high correlation with instrumental temperature (R^2 = 0.68 to 0.93; $p < 0.0001$). Despite periods of growth cessation/slowdown, mean seawater temperatures and annual ranges were reconstructed accurately. As demonstrated here, seawater temperature can be reconstructed with a maximum uncertainty of ± 2.7 °C. Therefore, our study shows that oxygen isotope values from *P. vulgata* can be used for the reconstruction of paleoclimate and the season of shell collection.

Keywords: Palaeoclimate; Seasonality; Geochemistry; Shells; Growth patterns.

1. Introduction

Marine molluscs are usually found in archaeological sites worldwide (Colonese et al., 2011; Erlandson, 2001; Gutiérrez-Zugasti et al., 2011). Ancient shells can provide a wide range of information on past subsistence strategies (e.g. Ainis et al., 2014; Cuenca-Solana, 2015; Manne and Bicho, 2011; Vanhaeren and d'Errico, 2006), but they also serve as palaeoclimate archives (Andrus, 2011; Schöne et al., 2004; Surge et al., 2003). Many molluscs grow their shells in isotopic equilibrium with the surrounding environment. This means that during shell formation chemical signatures from the environment in which the shells were living are incorporated into the carbonate (Dettman et al., 1999). The oxygen isotope value ($\delta^{18}O_{shell}$) in shell carbonate is mainly

a function of both the temperature and the oxygen isotope composition of the ambient water experienced by the mollusc during shell formation (Wanamaker et al., 2006). Therefore, oxygen isotope signatures recorded in ancient shells can be potentially used for reconstruction of past seawater temperatures, but also for determination of subsistence strategies and settlement patterns of past populations through the study of season of shell collection (Burchell et al., 2013; Colonese et al., 2009; Culleton et al., 2009; Mannino et al., 2003).

However, before oxygen isotope based techniques are applied to archaeological material, it is necessary to understand how reliably modern representatives of the respective species record their environment by means of $\delta^{18}O_{shell}$ (see for example Hallmann et al., 2009; Prendergast et al., 2013). A range of kinetic factors (usually known as "vital effects") can disrupt isotopic equilibrium. For example, a systematic offset from isotopic equilibrium has been found in shells of various *Patella* species across the eastern Atlantic and the Mediterranean (Fenger et al., 2007; Ferguson et al., 2011). This offset is different between species, but also between localities, suggesting that physiological responses of limpets might be environmentally driven. Similarly, investigations on the topshell *Phorcus turbinatus* have shown that the same species can respond differently in different locations, displaying variable offsets (Colonese et al. 2009; Mannino et al., 2008; Prendergast et al., 2013). Therefore, it is important to test isotopic equilibrium on shells from the same region where archaeological shells are going to be used for the reconstruction of past seawater temperatures. Apart from vital effects, interpretation of shell oxygen isotope values in terms of seawater temperatures can be biased by environmental factors, such as the isotopic composition of the seawater ($\delta^{18}O_{water}$). Variations in the $\delta^{18}O_{water}$ of the oceans are influenced by global (e.g. ice melting) and local processes (e.g. precipitation/evaporation balance, freshwater

input, advecting or upwelling). At a local scale, surface water salinity and $\delta^{18}O_{water}$ are highly correlated, as they increase with evaporation and decrease with precipitation (Ravelo and Hillaire-Marcel, 2007). Given that $\delta^{18}O_{shell}$ is a function of both seawater temperature and $\delta^{18}O_{water}$, it is important to know the contribution of $\delta^{18}O_{water}$ to $\delta^{18}O_{shell}$ through calibration of modern shells and comparison with instrumental data. Finally, information on shell growth patterns (timing and rate of seasonal shell formation) is also crucial for a correct interpretation of isotopic data. Molluscs usually grow more slowly or even stop growing at different times of the year and for various different reasons (e.g. extreme temperatures, storms, spawning, etc.) (Schöne, 2008). During growth cessation environmental signals are not recorded by the shell, and therefore actual seawater temperatures can be under- and/or overestimated.

Northern Iberia is a key region for the study of long-term changes in hunter-fisher-gatherer societies. Numerous Upper Palaeolithic and Mesolithic sites have been recorded in the region, providing one of the richest archaeological records in the world for the study of the Pleistocene-Holocene transition. Shells of different species, such as *Phorcus lineatus* (da Costa, 1778), *Patella vulgata* Linnaeus, 1758 and *Patella depressa* Pennant, 1777 have been abundantly recorded at those archaeological sites. Among them, the limpet *P. vulgata* shows great potential for the study of long-term palaeoclimate sequences in this region, as this species is found in archaeological sites continuously from the Late Pleistocene to the Holocene. The first studies on shell oxygen isotopes from *P. vulgata* produced irregular patterns of environmental variations, probably due to sampling with coarse resolution (Craighead, 1995; Deith & Shackleton, 1986). Recently, high-resolution studies using modern and archaeological *P. vulgata* shells from Atlantic locations have confirmed the utility of this species for reconstruction of seawater temperatures and determination of growth patterns (Ambrose

et al., 2015; Fenger et al., 2007; Ferguson et al., 2011; Surge and Barrett, 2012; Wang et al., 2012). However, only Fenger et al. (2007) conducted a calibration on this species, using modern shells from northern England. Information derived from this study was used for interpretation of oxygen isotope records from shells recovered in archaeological sites from the United Kingdom (Surge and Barrett, 2012; Wang et al., 2012). Later investigations by Surge et al. (2013), including modern shells from northern Iberia, produced oxygen isotope records following the same seasonal variations as seawater temperatures, but this study was focused on growth patterns rather than on palaeoenvironmental reconstruction. Therefore, despite the existence of previous isotopic studies in the region using modern specimens, a proper calibration of the $\delta^{18}O_{shell}$ as a palaeotemperature proxy has not yet been performed for this species in northern Iberia.

In this paper, we test the ability of *P. vulgata* shells from northern Spain as a palaeoclimate archive through the study of oxygen isotope values from modern samples. This study includes a tighter control of variables than in previous research (Fenger et al., 2007; Surge et al., 2013) by including a more accurate seawater monitoring, different sampling approaches and a detailed sclerochronological analysis. Results are used to discuss isotopic equilibrium, growth patterns, and reconstruction of seawater temperatures. We also discuss the potential and limits of the method and its implications for palaeoclimate and archaeological studies. Calibration of $\delta^{18}O_{shell}$ from *P. vulgata* as a proxy for determination of seawater temperatures in northern Iberia is crucial to understand environmental conditions faced by hunter-fisher-gatherers during the Pleistocene and the Holocene, and also for reconstruction of subsistence strategies and settlement patterns.

2. Study area and environmental setting

The study area is located in the north of the Iberian Peninsula, known as the Cantabrian Coast (Fig. 1). The climate is oceanic, humid, and temperate, with mild winters and summers. This is partly determined by geographical elements such as the North Atlantic Current, which cause the temperature to be higher than expected for this latitude (ca. 43 °N). The mean annual atmospheric temperature is ~15 – 16 °C. January is the coldest month with an average temperature of 9 – 10 °C, and August the warmest month with 20 – 22 °C. The mean annual rainfall exceeds 1200 mm and shows a marked seasonality, with the wetter conditions in spring and autumn and the driest period coinciding with summer months (Source: Spanish National Meteorology Agency, http://www.aemet.es). The higher rainfall is a result of the Föhn effect because the mountains prevent the clouds from crossing inland to the Meseta in north-central Spain (Rasilla, 1999).

The Cantabrian Sea (southern Bay of Biscay) represents a boundary between subtropical and boreal conditions in the Eastern Atlantic. The area is dominated by semidiurnal tidal cycles (two high tides and two low tides every lunar day). Sea surface temperatures follow a seasonal warming and cooling pattern, ranging from ca. 22 °C to ca. 12 °C in the central part of the region (i.e. Santander, data from the Spanish Institute of Oceanography). Hydrographic conditions throughout the year follow a regular pattern characterised by winter mixing and summer stratification. Wind-induced upwelling events, which are characterised by low temperatures, high salinity, and nutrient concentrations, have been observed to occur mainly in summer (Álvarez et al., 2011; Lavín et al., 1998). The water related to these upwelling events in the region is generally Eastern North Atlantic Central Water (ENACW), which is a cold and salty

water mass. However, some authors have also detected winter upwelling events associated with the Iberian Poleward Current (Gil et al., 2002) and with shelf bottom seawater (see Álvarez et al., 2011 and references therein).

3. Biology and ecology of *P. vulgata*

The limpet *P. vulgata* Linnaeus, 1758 inhabits the intertidal rocky shore from northern Norway to southern Portugal (Poppe and Goto, 1991). This species is adapted to cold water conditions and it is able to survive a wide range of atmospheric temperatures (from -9 °C to 43 °C) (Crisp, 1965; Branch, 1981). However, according to its geographical distribution, ideal conditions for *P. vulgata* development comprise seawater temperatures from ca. 8 °C to 19 °C and sea surface salinity from 20 to 35 psu (Fretter and Graham, 1976). Recent studies showed that thermal stress levels in *P. vulgata* are not primarily related to elevated air temperatures, but directly linked to elevated water temperature, showing an upper threshold of 23 °C (Seabra et al., 2016).

Growth rates on *P. vulgata* vary greatly, ranging from ~1.5 mm/year (Blackmore, 1969) to 4.4 mm/year (Jenkins and Hartnoll, 2001) for individuals sized between 25 and 35 mm. The longevity of this animal is highly dependent on the environmental conditions and has been reported to be up to ca. 16 years (Fischer-Piette, 1941). By comparison, a recent oxygen isotope study of specimens from northern England reconstructed a lifespan of up to ca. 8 years (Fenger et al., 2007). Studies on the Atlantic coasts of northern Iberia have identified a period of gonad activity between late spring and late autumn. Gonad indices (i.e. the ratio between gonadal and foot wet weight) reached maxima in October and November, but also showed some evidence of re-ripening in winter. The main spawning events have been identified between

November and January (Fernández et al., 2015; Guerra and Gaudencio, 1986; Ibañez et al., 1986; Miyares, 1980). Understanding reproduction is important for the interpretation of growth patterns, as molluscs need to expend more energy during the reproduction cycle, reducing the amount of energy available for growth (Crothers, 1994; Schöne et al., 2008).

The characteristics of mineralogy and microstructure of *P. vulgata* have been previously reported (McClintock, 1967). Two layers have been found interior to the myostracum (i.e. the muscle attachment): (1) a calcitic, radial crossed-foliated layer (m-2); and (2) an aragonitic, radial crossed-lamellar layer (m-1). Three additional layers have been identified exterior to the myostracum: (1) an aragonitic, concentric crossed-lamellar layer (m + 1); (2) a calcitic, concentric crossed-foliated layer (m + 2); and (3) a calcitic, radial crossed-foliated layer (m + 3) (Fig. 2A).

4. Material and methods

4.1 Modern shells and sampling procedure

Some 243 modern specimens of *P. vulgata* were gathered during 19 collection events between the 12th October 2011 and the 1st October 2012 from the intertidal rocky shore of Langre Beach (Cantabria, Northern Spain, Fig. 1). The soft parts of the limpets were removed immediately after collection. To clean the shells, they were immersed in H_2O_2 (30%) and de-ionized H_2O (70%) solution for 48 h, they were air-dried at ambient temperature, then cleaned in an ultrasonic bath for 5 min, and finally air-dried again at ambient temperature.

Two sampling strategies were followed in order to obtain two different datasets. In the first sampling strategy, shell edge samples were used to test for isotopic equilibrium and check how well instrumental (T_{meas}) and calculated temperatures ($T_{\delta 18O}$) match. Using this method, isotopic values corresponding to the last day/s of shell growth can be accurately associated with instrumental temperatures recorded at the time of shell collection. For this purpose, one carbonate sample was taken from the inner part of the shell aperture from every limpet. Six limpets from each of the 19 collection events were sampled, providing a total of 114 powder samples for oxygen isotope analysis. Approximately 200 μg of carbonate powder was obtained by milling along the perimeter of the innermost part of the shell-edge with the aid of a manual diamond drill (Fig. 2A). The sampled area represents the last portion of shell carbonate secreted by the animal and corresponds to the calcite concentric crossed-foliated layer (m + 2). Oxygen isotope values of shell-edge samples were measured using a Thermo Finnigan MAT 253 dual inlet isotope ratio mass-spectrometer coupled to a Finnigan Kiel IV carbonate device at the Instituto de Geociencias CSIC-UCM (Madrid). All these samples were compared to a reference carbon dioxide obtained from the calcite international standards NBS-18 and NBS-19. Replicate analyses of one sample out of 10 to 15 samples confirmed that the analytical precision of the instrument was better than ± 0.1 ‰. In the second sampling strategy, sequential samples were used to corroborate the accuracy of reconstructed temperatures and to determine growth patterns through sclerochronology. Sequential micro-sampling was carried out along the shell posterior side (from the shell aperture to the apex) of four modern individuals collected on 1st October 2012 (two from the high shore and two from the low shore) in order to obtain a high resolution isotope record. Two thick sections were produced from each limpet shell following the procedure described by Schöne et al. (2005). Shells were mounted on metal cubes with

Araldite glue and covered with a protective layer of metal epoxy (JB-Kwik) to prevent shells from breakage during cutting. Two 3 mm-thick sections were cut along the axis of maximum growth (Figs. 2B and 2C) using a low speed saw (Buehler IsoMet 1000) equipped with a 0.5 mm thick diamond-disc saw. Thick-sections were mounted on glass slides and ground with F600 and F800 grit SiC powder for 5 and 3 minutes, respectively. Additionally, each section was polished for ca. 6 minutes with 1μm Al_2O_3 powder. All samples were cleaned ultrasonically in ultrapure water to remove grinding and polishing powder. Finally, they were rinsed with freshwater and air-dried for at least 24 hours. One polished section of each specimen was used for micromilling carbonate powders using a New Wave Micromill equipped with a 1 mm conical SiC dental drill bit (Brasseler) in order to analyse oxygen isotope values, while the other section was used for growth pattern analysis. Limpets were sub-sampled by micromilling sample powders (following sample paths of ca. 70 – 200 μm in width, and 300 – 400 μm in depth) from the limpet shell margins toward the apex thereby achieving sub-monthly resolution. Sampling was conducted following the growth increments from the outer to the inner surface of the limpet (Fig. 2D). Between 125 and 200 μg of calcium carbonate powder was obtained for each sample. The sampled area corresponded to the calcitic concentric crossed-foliated (m + 2) and calcitic radial crossed foliated (m + 3) *P. vulgata* calcite layers, which were targeted to avoid the mixture between calcite and aragonite layers (e.g. MacClintock, 1967; Fenger et al., 2007; Ortiz et al., 2009; Demarchi et al., 2013). The milled powder from the four modern specimens that were sampled sequentially was loaded into 12 ml Exetainer ® tubes, and oxygen isotope values were determined by online phosphoric acid digestion at 70°C using a Thermo GasBench 2 preparation system coupled to a Thermo Delta V Advantage stable-isotope-ratio mass spectrometer in the Stable Isotope Facility at the

University of Bradford, UK. Standardisation of $\delta^{18}O$ values against the V-PDB reference frame was undertaken using repeated measurements of international standards NBS-19 and IAEA-CO-1, as well as two laboratory standards depleted in ^{18}O. The analytical precision of the instrument was better than ± 0.1 ‰.

For both isotope ratio mass spectrometry techniques (shell edges and shell sampled sequentially), oxygen isotope data are reported in the standard delta (δ) notation in parts per thousand (‰) relative to the international VPDB standard, with the $\delta^{18}O$ composition of seawater quoted relative to VSMOW.

4.2 Predicted $\delta^{18}O_{shell}$ and reconstructed temperatures

In order to test for isotopic equilibrium, we compared $\delta^{18}O$ values from the shell edge ($\delta^{18}O_{shell}$) with predicted $\delta^{18}O$ values calculated from seawater temperatures and $\delta^{18}O_{water}$. Predicted values were calculated using the equilibrium fractionation equation for calcite and water proposed by Friedman and O'Neil (1977):

$$1000\ln\alpha = 2.78 \times 10^6/T^2 - 2.89 \quad (1)$$

where T is the temperature measured in Kelvin and α is the fractionation between water and calcite described by the equation:

$$\alpha = (1000+\delta^{18}O_{shell}\ (SMOW))/(1000+\delta^{18}O_{water}\ (SMOW)) \quad (2)$$

Reconstructed seawater temperatures ($T_{\delta 18O}$) were derived from $\delta^{18}O_{shell}$ values using the mean seasonal $\delta^{18}O_{water}$ and equations (1) and (2).

4.3 Sclerochronolgy

For growth pattern analysis, one of the two polished sections of each specimen was immersed in Mutvei's solution for ca. 20 min under constant stirring at 37 – 40 °C in order to enhance the visibility of shell growth lines and increments (Schöne et al., 2005). This technique allows the identification of minor and major growth lines and increments (i.e. fortnightly, circadian, circalunidian) (Fig. 2E). Stained surfaces of the thick-sections were photographed with a Canon EOS 550E mounted on a binocular microscope (Wild Heerbrugg) equipped with a sectoral dark field illumination (VisiLED MC 1000). Photographs were assembled with ICE software (Image Composite Editor ©Microsoft). Circalunidan widths were measured to the nearest 1 µm in the direction of growth using the image processing software Panopea (© Peinl and Schöne).

Predicted $\delta^{18}O_{shell}$ values were also used to temporally align $\delta^{18}O_{shell}$ values from the four limpets sampled sequentially. Temporal alignment of the oxygen isotope record was performed taking into account data on major growth lines, as well as on fortnightly and circalunidian growth increments and lines (Fig. 2E). Major growth lines were used as a reference for anchoring the $\delta^{18}O_{shell}$ values. The first sample after a major growth line was anchored to the corresponding predicted value. The remaining points were aligned with the predicted time series by counting the number of circalunidian increments to the next major growth line.

4.4 Environmental parameters: $\delta^{18}O_{water}$ and salinity

In order to aid in the interpretation of modern shell $\delta^{18}O$ values, seawater chemistry ($\delta^{18}O_{water}$) and salinity (S_{meas}) were characterised. Seventy water samples were collected at four locations around the study area contemporaneously with shell collection. Locations were chosen to follow a spatial gradient from fully marine to fully freshwater sources: Langre Beach (open coast), Somo (estuary), Astillero (estuary) and La Cavada (Miera river) (Fig. 1). Comparison between locations was used to establish whether shells collected from Langre were affected by freshwater input. Water samples were collected in airtight polyethylene bottles (HDPE) with no headspace, so no air bubbles got trapped inside the bottle, and then stored in a standard refrigerator at ca. 4 °C. Samples were analysed using an IRMS Thermo Delta V coupled to a Gas Bench II at Cornell University (USA). To calibrate the instrument, both standard samples and international samples from the Atomic Energy International Association were used. The results were reported in relation to the international standard, Vienna Standard Mean Ocean Water (VSMOW ‰) and in δ notation. The analytical precision of the instrument was 0.17‰. Salinity (S_{meas}) was measured using a conductivity meter WTW Cond 330i at the University of Cantabria (Spain), and results are presented in practical salinity units (PSU).

4.5 Instrumental data

Instrumental data on seawater temperature (daily T_{meas}) for the period of collection were obtained from El Bocal station (Santander), property of the Aquaculture Research Facility of the Spanish Institute of Oceanography (http://www.ieo-santander.net/), located ca. 11 km away from the sampling area (Fig. 1). The mean annual T_{meas} calculated from daily temperatures recorded at the time of shell collection

was 15.6 °C. Temperatures were colder in February (11.2 °C), and warmer in August (20.8 °C) (Fig. 3). T_{meas} on the day of each collection event was used for the calculation of predicted $\delta^{18}O$ values at the shell edges, while daily T_{meas} were used for calculation and time calibration of predicted $\delta^{18}O$ values of shells sampled sequentially, as well as for comparison with reconstructed $T_{\delta 18O}$. The amount of monthly precipitation over the study area ranged from 255 mm (April) to 27 mm (July) during the period from October 2011 to October 2012 (Source: National Meteorology Agency, http://www.aemet.es) (Fig. 3).

5. Results

5.1 Seawater chemistry and salinity

Important differences were observed in $\delta^{18}O_{water}$ and S_{meas} values between locations (Fig. 4; Table 1). Lower values were found in autumn, winter and spring, while higher values corresponded to the summer. Small seasonal variations in $\delta^{18}O_{water}$ were found to occur at open coast and freshwater locations such as Langre and La Cavada, respectively, while larger changes in $\delta^{18}O_{water}$ were found at the two estuarine locations, Somo and Astillero (Fig. 4). While $\delta^{18}O_{water}$ and S_{meas} data across all four locations showed a strong correlation (R^2= 0.97; $p < 0.0001$), individual localities showed weaker correlations. Only estuarine locations showed a strong correlation (R^2= 0.94; $p < 0.0001$ and 0.62; $p = 0.0001$ for Somo and Astillero, respectively), while correlation at Langre was very low (R^2= 0.25; $p = 0.02$).

5.2 Shell oxygen isotopes ($\delta^{18}O_{shell}$)

Intra-annual $\delta^{18}O_{shell}$ from shell edges exhibited distinct seasonal fluctuations throughout the year, but also some variability between samples from the same collection event (Fig. 5). Comparison between measured $\delta^{18}O_{shell}$ and predicted $\delta^{18}O_{shell}$ showed a high correlation (R^2= 0.93; p < 0.0001), suggesting isotopic equilibrium with the surrounding environment during shell growth (Fig. 6). However, a mean annual offset of 0.36 ‰ between measured and predicted $\delta^{18}O_{shell}$ was identified. When using mean annual $\delta^{18}O_{water}$ values seasonal differences were recorded, with the highest offset in summer months, but when calculations were performed using monthly $\delta^{18}O_{water}$ values the offset was rather stable throughout the year, with only a slightly lower offset recorded in winter (Table 2).

The four limpets sampled sequentially also showed clear seasonal variations (Fig. 7). Maximum and minimum $\delta^{18}O_{shell}$ values, as well as the annual range, were rather similar among the four specimens, and in agreement with results from the shell edges. Only the shell LAN25 exhibited considerably more negative summer values (up to −0.70‰), and therefore a larger annual range than the other shells. Annual cycles of the sampled shells ranged from one and a half to four and a half years (Table 3). Measured and predicted $\delta^{18}O_{shell}$ values were in good agreement, and showed a strong correlation in the four limpets (R^2 = from 0.72 to 0.93; p < 0.0001) (Fig. 8).

5.3 Reconstructed temperatures ($T_{\delta 18O}$)

The mean annual offset (0.36 ‰) was subtracted from measured $\delta^{18}O_{shell}$ values in order to calculate seawater temperatures. Reconstructed $T_{\delta 18O}$ from all shell edge samples ranged from 10.7 °C to 20.6 °C (annual range = 9.9 °C), while mean calculated

$T_{\delta 18O}$ for each collection event ranged from 11.8 °C to 20 °C (annual range = 8.2 °C). Thus, reconstructed $T_{\delta 18O}$ for each collection event was very similar to instrumental temperatures (T_{meas}), showing high correlations (R^2 = 0.93; $p < 0.0001$) (see Table 4; Fig. 9). Instrumental temperatures were within one standard deviation of mean reconstructed temperatures. Exceptions to this can be seen in temperatures recorded on 5 August 2012 and 24 December 2011 (Fig. 9). Although mean annual values were the same for T_{meas} and $T_{\delta 18O}$, these dates saw maximum positive and negative offsets of 1.9 and −1.6°C, respectively (Table 4).

Reconstructed $T_{\delta 18O}$ from the four shells sampled sequentially was also in good agreement with T_{meas} and $T_{\delta 18O}$ from shell edges. Results showed similar patterns, with minimum (11.3 °C, 12.2 °C, 10.9 °C and 11.9 °C) and maximum (24.9 °C, 22 °C, 20.9 °C and 22.2 °C) temperatures producing mean annual ranges between 9.8 °C and 13.6 °C (Table 5). $T_{\delta 18O}$ correlated strongly with T_{meas} (R^2= from 0.68 to 0.93; $p < 0.0001$) (Fig. 10).

5.4 Sclerochronology

Growth pattern analysis was conducted on the sections of the four shells that were sampled sequentially. Major (annual) and minor (fortnightly and circalunidian) growth lines and increments were identified in all shells. Major growth lines were related to significant growth cessation and were characterised by a change in the orientation of the micro-growth increments (which usually leads to the formation of a notch in the surface of the outer shell), as well as the overlapping of new growth over the stop line (Fig. 11C). Minor growth increments consisted of micro-growth increments separated by micro-growth lines. Two types of minor increments and lines

were identified: a) periodic bundles containing 14–15 micro-growth increments and lines (fortnightly), and b) lunar daily growth increments and lines (circalunidian) (Fig. 11C, D). Counting of circalunidian increments in portions of shell growth matched very well the number of days represented in those portions, suggesting that growth lines and increments were formed with circatidal periodicity (Fig. 11A-E). Prominent growth lines and narrower increments were formed during spring tides (full and new moon), while neap tides (first and last quarter) formed narrower growth lines (sometimes barely visible) and wider growth increments (Fig. 11E).

Counting and measuring lunar daily increments allowed for a detailed interpretation of growth patterns and determination of periods of growth cessation. Hence, shells LAN25, LAN43 and LAN45 put on new growth during 50–60 % of the available days during the course of their lives. However, LAN29 showed a much higher growth rate, growing ~80 % of the days (Table 6). Variable seasonal growth patterns were recorded, with the fastest growth rates mainly occurring in spring months, and the longest periods of growth cessation/slowdown occurring in summer and winter (Fig. 8). Nevertheless, shorter periods of growth cessation/slowdown were also identified in spring and autumn (e.g. spring 2010 and autumn 2011 from LAN43).

In addition, the temporal alignment of the isotope data showed that our sampling strategy achieved weekly resolution (mean number of days per isotope sample = ~6) in the younger portions of the shells, where the sampling surface is wider. In the older portions of the shell, where the sampling surface is narrower and larger sampling paths are needed, our sampling strategy achieved fortnightly resolution (Table 6).

6. Discussion

6.1 Seawater chemistry and salinity

In general terms, lower values, in both $\delta^{18}O_{water}$ and S_{meas}, corresponded to the time interval of enhanced freshwater input due to greater rainfall in the area (autumn, winter and spring), while higher values were probably due to evaporation during both the drier season (i.e. summer) and periods of shorter rainfall in autumn and spring. Changes in both parameters throughout the year were much more marked in estuarine locations due to the effect of freshwater input. Results from seawater chemistry and salinity suggest that fully marine conditions existed at Langre beach at the time of shell collection. Small variations, in both $\delta^{18}O_{water}$ and S_{meas}, at Langre are likely explained by influx of meteoric waters (i.e. precipitation, run-off…) during periods of greater rainfall (Table 1). Absolute values recorded at this location were lower than those reported for Mediterranean locations such as Gibraltar (Max = 1.67 ‰, Min = 0.99 ‰, see Ferguson et al., 2011) and Malta (Max = 1.60 ‰, Min = 1.10 ‰, see Prendergast et al., 2013), but all of them showed a very similar range (0.64 ‰ in Langre and 0.68 ‰ and 0.50 ‰ in Gibraltar and Malta, respectively).

6.2 Isotopic equilibrium

Results indicate that shells grew close to isotopic equilibrium with the surrounding environment. Measured and predicted $\delta^{18}O_{shell}$ values showed a high correlation, although a mean annual offset of 0.36 ‰ was identified. Previous studies have reported positive offsets in *Patella* species. A positive offset of 1.01 ‰ was found in *P. vulgata* from northern England (Fenger et al., 2007), 0.72 ‰ in *P. caerulea* and *P. rustica* from Gibraltar (Ferguson et al., 2011), and 0.70 ‰ in *Patella tabularis* from

South Africa (Cohen and Tyson, 1995; Shackleton, 1973). Moreover, Schifano and Censi (1983) also recorded a positive offset in *Patella caerulea* from Sicily (Italy). However, the offset found in our study (0.36 ‰, corresponding to ca. 1.8 °C) is considerably lower than those reported previously. According to recent investigations (Ferguson et al., 2011; Prendergast et al., 2013; Schöne et al., 2007) the magnitude of the offset in marine shells strongly depends on the $\delta^{18}O_{water}$ value used. Therefore, the reduced offset obtained in our study is probably related to the use of temporally highly-resolved $\delta^{18}O_{water}$ data. Nevertheless, although using high resolution $\delta^{18}O_{water}$ data was useful to reduce the offset, its potential causes (e.g. the type of magnesium incorporated, vital effects – kinetic and metabolic –, and micro-environmental factors), and the associated factors and mechanisms are still unknown (Fenger et al., 2007). However, as this offset from isotopic equilibrium is predictable, seawater temperatures can be accurately calculated by substracting the offset from the $\delta^{18}O_{shell}$ values.

6.3 Reconstructed seawater temperatures ($T_{\delta 18O}$)

Seawater temperatures reconstructed from the oxygen isotope record were in very good agreement with instrumental temperatures (Fig. 10). Significant deviations of reconstructed temperatures from instrumental temperatures were only identified in summer 2009 and summer/autumn 2010 of LAN25, and they were probably due to desiccation stress experienced by this limpet as a result of living high on the shore.

Results from shell edge samples revealed lower $T_{\delta 18O}$ than T_{meas} during summer months, probably due to growth cessation/slowdown. Isotopic and sclerochronological data from sequential shell samples also showed summer growth cessation/slowdown, suggesting that reconstructed summer temperatures might be underestimating measured

temperatures. However, high growth rates were also recorded in the warmer periods of the year in some shells (e.g. LAN25 in 2009 and 2010, LAN29 and LAN43 in 2011), suggesting that seawater temperatures were correctly estimated for those summers. A similar process has been identified in winter. Thus, provided several annual cycles are available for interpretation, summer and winter seawater temperatures and annual ranges can be accurately reconstructed.

The $\delta^{18}O_{shell}$ of the shell edge samples showed good correlation with predicted $\delta^{18}O_{shell}$ ($R^2 = 0.93$; $p < 0.0001$), but not with $\delta^{18}O_{water}$ ($R^2 = 0.03$; $p = 0.49$).This implies that the contribution of $\delta^{18}O_{water}$ to $\delta^{18}O_{shell}$ was negligible, and therefore $\delta^{18}O_{shell}$ was mainly a function of seawater temperature. Nevertheless, the amplitude of the $\delta^{18}O_{water}$ should be taken into consideration when calculating temperatures. In order to test whether the $\delta^{18}O_{water}$ annual range observed in Langre Beach (0.64 ‰) impacted on the temperature calculation, we calculated $T_{\delta 18O}$ using $\delta^{18}O_{water}$ values at the time of collection, mean annual values, and maximum and minimum annual values. Results showed a difference of ca. ± 1.4 °C when using mean annual rather than collection event $\delta^{18}O_{water}$ values, and a difference of ca. ± 2.8 °C when maximum and minimum values are used (Table 7). When the analytical precision of the IRMS (± 0.5 °C) and the average standard deviation (± 0.8 °C) are added, results suggest that in northern Iberia past $T_{\delta 18O}$ can be calculated with a maximum uncertainty of ± 2.7 °C. Similar uncertainty has been reported for other species (Gutiérrez-Zugasti et al., 2015; Prendergast et al., 2013).

6.4 Growth patterns

Combining oxygen stable isotopes and sclerochronology assisted in establishing growth patterns. Inter- and intra-shell variations in the duration and intensity of the growth cessation/slowdown were observed in *P. vulgata* shells. Differences in growth patterns are very well exemplified in the summer of 2011 (Fig. 8). No growth at all was recorded in the shell LAN25 from early June to early November (five months), growth cessation was restricted to August (one month) in LAN29, while LAN43 grew uninterruptedly throughout the warmer season, and LAN45 showed growth cessation from August to late October (three months). Similar variations were recorded throughout the remainder of associated $\delta^{18}O_{shell}$ series. Therefore, our study shows a general ontogenetic trend toward growth cessation/slowdown in summer and winter, but also suggests the occurrence of high intra-specific variability in growth patterns of the limpet *P. vulgata*. In addition, the average width of the lunar daily growth increments was very homogeneous in the four limpets (~13 µm) (Table 5), showing no clear seasonal trends (Fig. 8), which suggests that differences in growth rates between shells were related to the duration of growth cessation/slowdown rather than to the occurrence of seasonal periods of maximum and minimum growth.

Intra-specific variability also prevented a clear identification of the mechanisms driving shell growth cessation/slowdown. Shell growth in molluscs usually stops or slows down when temperatures are higher or lower than their optimal thermal tolerance, demanding that most of the available energy is dedicated to survival under those unfavourable conditions (Schöne, 2008). In our case, thermal tolerance might be responsible for growth cessation/slowdown in summer and winter, when maximum and minimum temperatures are recorded in northern Iberia. Recently, the upper threshold of thermal tolerance for *P. vulgata* has been established as 23 °C (Seabra et al., 2016). In our study, when shells grew during summer, they generally reflected maximum

temperatures of up to ~22 °C, in agreement with instrumental temperatures. However, when shells exhibited summer growth cessation/slowdown, this process started with seawater temperatures of ~19 °C (Fig. 10). In the case of winter, thermal tolerance is not the only possible explanation for growth cessation/slowdown. The limpet *P. vulgata* is commonly reported as a species well adapted to cold climates, tolerating seawater temperatures down to 8 °C (Fretter and Graham, 1976). Nevertheless, our study area is located close to the southern geographical limit of the species (Poppe and Goto, 1991), and local seawater temperatures rarely drop below 11 °C. Therefore, limpets would not be expected to suffer thermal stress in winter at this latitude. In our study, when winter growth cessation/slowdown occurred, limpets stopped growing at 12–13 °C (Fig. 10), which might be implying that winter thermal stress starts at higher temperatures in southern locations. However, other factors, such as higher energy expenditure during periods of physiological activity, have been reported to lead molluscs to reduce growth rates. For example, spawning occurs in northern Iberia between November and January (Fernández et al., 2015; Guerra and Gaudencio, 1986; Ibañez et al., 1986; Miyares, 1980), and therefore might be responsible for growth/cessation in winter. Other biological factors (e.g. gametogenesis, which occurs between October and November in this region) and/or environmental conditions (e.g. short and dramatic environmental events, such as storms) might also be the source of shorter periods of growth cessation/slowdown recorded in spring and autumn.

Similar growth patterns have been previously recorded in modern *P. vulgata* shells. Fenger et al. (2007) reported limited winter growth in limpets from northern England. Surge et al. (2013) used isotope sclerochronology to identify the seasonal timing of annual growth line formation (i.e. the periods of growth cessation/slowdown) in shells from the cold- and warm-temperate zones and at the boundary between these

zones in the Eastern Atlantic. They found growth cessation/slowdown in winter in the cold zone (northern England), in summer in the warm-temperate zone (northern Iberia), and in both seasons in the boundary zone (southern England). Our study demonstrates slightly different results for northern Iberia, as growth cessation largely coincides with summer and winter (and also with spring and autumn, although much more sporadically). Therefore, using a combined isotopic and sclerochronological approach, more complex growth patterns emerged.

6.5 Implications for palaeoclimate and archaeology

Our study suggests that seawater temperatures can be accurately deduced from oxygen isotope ratios of limpet shell carbonate. However, when it comes to reconstruction of past climate, calculation of past seawater temperatures is not so straightforward. In the first place, the seasonal isotopic composition of the past seawater is unknown. According to some studies, this issue can be successfully approached by using a combination of isotopic and elemental analysis (e.g. Mg/Ca ratios) for reconstruction of past $\delta^{18}O_{water}$ (Bougeois et al., 2014; Ferguson et al., 2011). However, other studies suggest that no relationship exists between seawater temperatures and Mg/Ca ratios, and therefore they should not be used as palaeothermometers or for reconstruction of past $\delta^{18}O_{water}$ (Graniero et al., 2016; Poulain et al., 2015). In the case of the limpets, contradictory information has been recently published. Ferguson et al. (2011) and Cobo et al. (2017) found good correlation between Mg/Ca ratios and seawater temperatures on limpets from Iberia, while Graniero et al. (2016) reported no correlation for limpets from northern England and Tierra del Fuego. Results from these investigations suggest that the relation between elemental incorporation and seawater

temperatures might be site specific, and thus the utility of elemental ratios as a palaeonvironmental proxy should be locally tested. Reconstruction of past $\delta^{18}O_{water}$ can also be approached through the study of oxygen isotopes from carbonates of other marine organisms, such as planktonic foraminifera (Elderfield and Ganssen, 2000) and alkenones (Sikes and Volkman, 1993), or from pore water extracted from marine sediments (Schrag et al., 2002). The rate of freshwater discharge from the poles due to glacial melting has also been used to estimate $\delta^{18}O_{water}$ (Fairbanks, 1989). However, these methods do not provide seasonal records as in the case of Mg/Ca, but mean annual estimates of past $\delta^{18}O_{water}$ (Prendergast et al., 2013), leading to a slightly less precise calculation of past seawater temperatures.

In addition to the unknown isotopic composition of the seawater, other factors should be taken into account. For example, growth patterns of ancient limpet shells in the region may have differed during the Pleistocene and Early Holocene. Thus, modern limpet shells from different latitudes across the Eastern Atlantic Façade have been reported to show variable responses in terms of growth patterns (Surge et al., 2013). Similarly, limpets from northern Iberia living under the colder conditions of the Late Pleistocene would be expected to show growth patterns more similar to those recorded in northern England today, with growth cessation/slowdown in the winter months (Fenger et al., 2007).

Finally, the identification of periods of growth cessation/slowdown has important implications for interpretation of the season of shell collection. Our results indicate that long periods of time are missing from the growth record in shells of *P. vulgata* (mainly summer and winter), and accordingly it is not possible to obtain monthly or sub-monthly resolution when assessing the time of harvest of archaeological shells. However, periods of growth cessation in *P. vulgata* occur only during certain

seasons and are usually less than three months in duration, so that reconstruction of seasonality of shell collection can be accurately established for archaeological samples with certain limits.

7. Conclusions

Shell oxygen isotope values of modern *P. vulgata* collected in northern Iberia during 2011 and 2012 were calibrated against seawater temperatures to establish their reliability as a palaeotemperature proxy. Results showed that limpets precipitated carbonate to form their shells close to isotopic equilibrium, with a predictable (and therefore rectifiable) mean offset between observed and predicted values of 0.36 ‰ (equivalent to ~1.8 °C). Limpet shells showed higher growth rates in spring, and a growth cessation/slowdown in summer and winter. Despite this, our study recorded high intra-specific variability (both between and within shells) in growth patterns. Reconstructed seawater temperatures exhibited high correlation with instrumental temperatures, although in some annual cycles a seasonal growth cessation was likely responsible for underestimation of temperatures. Nevertheless, when several annual cycles were preserved in shell growth patterns, mean seawater temperatures and annual ranges were reconstructed accurately. A study of the effect of $\delta^{18}O_{water}$ amplitude on $\delta^{18}O_{shell}$-based temperature reconstruction showed that seawater temperatures can be reconstructed with a maximum uncertainty of ± 2.7 °C. Our study also has implications for archaeological research into wider issues. Paleoclimate and seasonality of shellfish collection are key factors for the interpretation of subsistence strategies, social organisation and mobility patterns of hunter-fisher-gatherers from northern Iberia. Our demonstration that a combined isotope and sclerochronological analysis can be used to

infer with confidence seasonal shellfish collection patterns is a major contribution to these wider interpretations.

Acknowledgements

This research was part of the projects NF100413 (Newton International Fellowship granted to IGZ) and HAR2013-46802-P (funded by the Spanish Ministry of Economy and Competitiveness). IGZ was also supported by the Juan de la Cierva Research Programme (grant number JCI-2012-12094) funded by the Spanish Ministry of Economy and Competitiveness (MINECO). RSR is supported by a predoctoral contract from the Plan Estatal de Investigación Científica y Técnica y de Innovación 2013-2016 (grant number BES-2014-070075), co-funded by the Spanish Ministry of Economy and Competitiveness (MINECO), the Servicio Público de Empleo Estatal and the Fondo Social Europeo. The Servicio de Actividades Pesqueras of the Government of Cantabria provided authorisation for collection of modern specimens. Salinity was measured by José Ramón Mira Soto at the Departamento de Ciencias y Técnicas del Agua y del Medio Ambiente of the Universidad de Cantabria. The University of York, the University of Bradford, the University of Mainz, the University of Cantabria, as well as the IIIPC (Cantabrian International Institute for Prehistoric Research), and the Instituto de Geociencias CSIC- UCM provided facilities and technical support, while the Spanish Institute of Oceanography (Santander Oceanographic Centre) kindly provided data on seawater temperatures. We would also like to thank Carl Heron, Donna Surge, Tracy Fenger, Julie Ferguson, André Colonese, Javier Martín-Chivelet and Asier García-Escárzaga for their help and comments during the course of this research.

References

Ainis, A.F., Vellanoweth, R.L., Lapeña, Q.G., Thornber, C.S., 2014. Using non-dietary gastropods in coastal shell middens to infer kelp and seagrass harvesting and paleoenvironmental conditions. Journal of Archaeological Science 49, 343-360.

Álvarez, I., Gómez-Gesteira, M., Decastro, M., Lorenzo, M.N., Crespo, A.J.C., Dias, J.M., 2011. Comparative analysis of upwelling influence between the western and northern coast of the Iberian Peninsula. Continental Shelf Research 31, 388-399.

Ambrose, W.G., Locke V, W.L., Bigelow, G.F., Renaud, P.E., 2015. Deposition of annual growth lines in the apex of the common limpet (*Patella vulgata*) from Shetland Islands, UK and Norway: Evidence from field marking and shell mineral content of annual line deposition. Environmental Archaeology 21, 79-87.

Andrus, C.F.T., 2011. Shell midden sclerochronology. Quaternary Science Reviews 30, 2892-2905.

Blackmore, D.T., 1969. Studies of *Patella vulgata* L. I. Growth, reproduction and zonal distribution. Journal of Experimental Marine Biology and Ecology 3, 200-213.

Bougeois, L., De Rafélis, M., Reichart, G.-J., De Nooijer, L.J., Nicollin, F., Dupont-Nivet, G., 2014. A high resolution study of trace elements and stable isotopes in oyster shells to estimate Central Asian Middle Eocene seasonality. Chemical Geology 363, 200-212.

Burchell, M., Cannon, A., Hallmann, N., Schwarcz, H.P., Schöne, B.R., 2013. Inter-site variability in the season of shellfish collection on the central coast of British Columbia. Journal of Archaeological Science 40, 626-636.

Branch, G.M., 1981. The biology of limpets: physical factors, energy flow and ecological interactions. Oceanography and Marine Biology Annual Review 19, 235-380.

Cohen, A.L., Tyson, P.D., 1995. Sea-surface temperature fluctuations during the Holocene off the south coast of Africa: implications for terrestrial climate and rainfall. The Holocene 5, 304-312.

Colonese, A.C., Troelstra, S., Ziveri, P., Martini, F., Lo Vetro, D., Tommasini, S., 2009. Mesolithic shellfish exploitation in SW Italy: seasonal evidence from the oxygen isotopic composition of *Osilinus turbinatus* shells. Journal of Archaeological Science 36, 1935-1944.

Colonese, A.C., Mannino, M.A., Bar-Yosef Mayer, D.E., Fa, D.A., Finlayson, J.C., Lubell, D., Stiner, M.C., 2011. Marine mollusc exploitation in Mediterranean prehistory: an overview. Quaternary International 239, 86-103.

Craighead, A.S., 1995. Marine mollusca as palaeoenvironmental and palaeoeconomic indicators in Cantabrian Spain. Unpublished PhD Thesis, University of Cambridge, Cambridge, 485 pp.

Crisp, D.J., 1965. Observartions of the effect of climate and weather on marine communities. In: Johnson, C.G., Smith, L.P. (Eds.), The Biological Significance of Climatic Changes in Britain, Elsevier, New York, pp. 63-77.

Crothers, J.H., 1994. Student investigations on the population structure of the common topshell Monodonta lineata, on the Gore, Somerset. Field Studies 8, 337-355.

Cuenca-Solana, D., 2015. The Use of Shells by Hunter-Fisher-Gatherers and Farmers From the Early Upper Palaeolithic to the Neolithic in the European Atlantic Façade: A Technological Perspective. The Journal of Island and Coastal Archaeology 10, 52-75.

Culleton, B.J., Kennett, D.J., Jones, T.L., 2009. Oxygen isotope seasonality in a temperate estuarine shell midden: a case study from CA-ALA-17 on the San Francisco Bay, California. Journal of Archaeological Science 36, 1354-1363.

Deith, M., Shackleton, N., 1986. Seasonal exploitation of marine molluscs: oxygen isotope analysis of shell from La Riera cave. In: Straus, L.G., Clark, G.A. (Eds.), La Riera Cave. Stone Age hunter-gatherer adaptations in northern Spain, Arizona State University, Tempe, pp. 299-313.

Demarchi, B., Rogers, K., Fa, D.A., Finlayson, C.J., Milner, N., Penkman, K.E.H., 2013. Intra-crystalline protein diagenesis (IcPD) in *Patella vulgata*. Part I: Isolation and testing of the closed system. Quaternary Geochronology 16, 144-157.

Dettman, D.L., Reische, A.K., Lohmann, K.C., 1999. Controls on the stable isotope composition of seasonal growth bands in aragonitic fresh-water bivalves (unionidae). Geochimica et Cosmochimica Acta 63, 1049-1057.

Elderfield, H., Ganssen, G., 2000. Past temperature and d18O of surface ocean waters inferred from foraminiferal Mg/Ca ratios. Nature 405, 442-445.

Erlandson, J.M., 2001. The archaeology of aquatic adaptations: paradigms for a new millenium. Journal of Archaeological Research 9, 287-350.

Fairbanks, R.G., 1989. A 17,000-year glacio-eustatic sea level record: influence of glacial melting rates on the Younger Dryas event and deep-ocean circulation. Nature 342, 637-642.

Fenger, T., Surge, D., Schöne, B., Milner, N., 2007. Sclerochronology and geochemical variation in limpet shells (*Patella vulgata*): a new archive to reconstruct coastal sea surface temperature. Geochemistry, Geophysics, Geosystems 8, Q07001.

Ferguson, J.E., Henderson, G.M., Fa, D.A., Finlayson, J.C., Charnley, N.R., 2011. Increased seasonality in the Western Mediterranean during the last glacial from limpet shell geochemistry. Earth and Planetary Science Letters 308, 325-333.

Fernández, N., Alborés, I., Aceña-Matarranz, S., 2015. Characterization of the reproductive cycle and physiological condition of *Patella vulgata* in the NW of the Iberian Peninsula: relevant information for a sustainable exploitation. Fisheries Research 164, 293-301.

Fischer-Piette, E., 1941. Croissance, taille maxima et longévité possible de quelques animaux intercotidaux en fonction du milieu. Annales Institute Océanographique 21, 1-28.

Fretter, V., Graham, A., 1976. The Prosobranch molluscs of Britain and Denmark. Part 1: Pleurotomariacea, Fissurellacea and Patellacea. Journal of Molluscan Studies Supplement 1.

Friedman, I., O'Neil, J.R., 1977. Compilation of stable isotope fractionation factors of geochemical interest. In: Fleischer, M. (Ed.), Data of Geochemistry, United States Department of the Interior, Washington, pp. 1-12.

Gil, J., Valdés, L., Moral, M., Sánchez, R., Garcia-Soto, C., 2002. Mesoscale variability in a high-resolution grid in the Cantabrian Sea (southern Bay of Biscay), May 1995. Deep Sea Research Part I: Oceanographic Research Papers 49, 1591-1607.

Guerra, M.T., Gaudencio, M.J., 1986. Aspects on the ecology of *Patella* spp. on the portuguese coast. Hydrobiologia 142, 57-69.

Gutiérrez Zugasti, I., Andersen, S., Araújo, A.C., Dupont, C., Milner, N., Soares, A.M.M., 2011. Shell midden research in Atlantic Europe: state of the art, research problems and perspectives for the future. Quaternary International 239, 70-85.

Gutiérrez-Zugasti, I., García-Escárzaga, A., Martín-Chivelet, J., González-Morales, M.R., 2015. Determination of sea surface temperatures using oxygen isotope ratios from Phorcus lineatus (Da Costa, 1778) in northern Spain: implications for palaeoclimate and archaeological studies. The Holocene 25, 1002-1014.

Hallmann, N., Burchell, M., Schöne, B.R., Irvine, G.V., Maxwell, D., 2009. High-resolution sclerochronological analysis of the bivalve mollusk *Saxidomus gigantea* from Alaska and British Columbia: techniques for revealing environmental archives and archaeological seasonality. Journal of Archaeological Science 36, 2353-2364.

Ibáñez, M., Peña, J., Feliu, J., 1986. Reproduction of *Patella* spp. on the Basque coast of Spain. Hydrobiologia 142, 327.

Jenkins, S.R., Hartnoll, R.G., 2001. Food supply, grazing activity and growth rate in the limpet *Patella vulgata* L.: a comparison between exposed and sheltered shores. Journal of Experimental Marine Biology and Ecology 258, 123-139.

Lavín, A., Valdes, L., Gil, J., Moral, M., 1998. Seasonal and inter-annual variability in properties of surface water off Santander, Bay of Biscay, 1991-1995. Oceanologica Acta 21, 179-190.

Macclintock, C., 1967. Shell Structure of Patelloid and Bellerophontoid Gastropods (Mollusca), Peabody Museum of Natural History, Yale University, New Haven.

Manne, T., Bicho, N.F., 2011. Prying new meaning from limpet harvesting at Vale Boi during the Upper Paleolithic. In: Bicho, N.F., Haws, J., Davis, L.G. (Eds.), Trekking the Shore: Changing Coastlines and the Antiquity of Coastal Settlement, Springer, pp. 273-289.

Mannino, M.A., Spiro, B.F., Thomas, K.D., 2003. Sampling shells for seasonality: oxygen isotope analysis on shell carbonates of the inter-tidal gastropod

Monodonta lineata (da Costa) from populations across its modern range and from a Mesolithic site in southern Britain. Journal of Archaeological Science 30, 667-679.

Miyares, M.P., 1980. Biología de *Patella intermedia* y *P. vulgata* (Mollusca, Gasteropoda) en el litoral asturiano (N de España) durante un ciclo anual (Diciembre 1978 a Noviembre 1979). Boletín del Instituto de Estudios Asturianos 26, 173-192.

Ortíz, J.E., Torres, T., González Morales, M.R., Abad, J., Arribas, I., Fortea, F.J., García Belenguer, F., Gutiérrez Zugasti, I., 2009. The aminochronology of man-induced shell midden in caves in northern Spain. Archaeometry 51, 123-139.

Poppe, G.T., Goto, Y., 1991. European Seashells. Vol. I (Polyplacophora, Caudofoveata, Solenogastra, Gastropoda), Verlag Christa Hemmen, Germany.

Prendergast, A.L., Azzopardi, M., O'connell, T.C., Hunt, C., Barker, G., Stevens, R.E., 2013. Oxygen isotopes from *Phorcus* (*Osilinus*) *turbinatus* shells as a proxy for sea surface temperature in the central Mediterranean: a case study from Malta. Chemical Geology 345, 77-86.

Rasilla, D.F., 1999. Viento Sur y efecto Föhn en la Cordillera Cantábrica, CEDEX, Ministerio de Fomento, Madrid.

Ravelo, A.C., Hillaire-Marcel, C., 2007. Chapter Eighteen The Use of Oxygen and Carbon Isotopes of Foraminifera in Paleoceanography. In: Hillaire-Marcel, C., De Vernal, A. (Eds.), Proxies in Late Cenozoic Paleoceanography. Developments in Marine Geology, Volume 1, Elsevier, pp. 735-764.

Schifano, G., Censi, P., 1983. Oxygen isotope composition and rate of growth of *Patella coerulea*, *Monodonta turbinata* and *M. articulata* shells from the western coast of sicily. Palaeogeography, Palaeoclimatology, Palaeoecology 42, 305-311.

Schöne, B., 2008. The curse of physiology—challenges and opportunities in the interpretation of geochemical data from mollusk shells. Geo-Marine Letters 28, 269-285.

Schöne, B.R., Freyre Castro, A.D., Fiebig, J., Houk, S.D., Oschmann, W., Kröncke, I., 2004. Sea surface water temperature over the period 1884-1983 reconstructed from oxygen isotope ratios of a bivalve mollusk shell (*Arctica islandica*, southern North Sea). Palaeogeography, Palaeoclimatology, Palaeoecology 212, 215-232.

Schöne, B.R., Dunca, E., Fiebig, J., Pfeiffer, M., 2005. Mutvei´s solution: an ideal agent for resolving microgrowth structures of biogenic carbonates. Palaeogeography, Palaeoclimatology, Palaeoecology 228, 149-166.

Schöne, B.R., Rodland, D.L., Wehrmann, A., Heidel, B., Oschmann, W., Zhang, Z., Fiebig, J., Beck, L., 2007. Combined sclerochronologic and oxygen isotope analysis of gastropod shells (*Gibbula cineraria*, North Sea): life-history traits and utility as a high-resolution environmental archive for kelp forests. Marine Biology 150, 1237-1252.

Schrag, D.P., Adkins, J.F., Mcintyre, K., Alexander, J.L., Hodell, D.A., Charles, C.D., Mcmanus, J.F., 2002. The oxygen isotopic composition of seawater during the Last Glacial Maximum. Quaternary Science Reviews 21, 331-342.

Seabra, R., Wethey, D.S., Santos, A.M., Gomes, F., Lima, F.P., 2016. Equatorial range limits of an intertidal ectotherm are more linked to water than air temperature. Global Change Biology doi:10.1111/gcb.13321.

Shackleton, N.J., 1973. Oxygen isotope analysis as a means of determining season of occupation of prehistoric midden sites. Archaeometry 15, 133-141.

Sikes, E.L., Volkman, J.K., 1993. Calibration of alkenone unsaturation ratios (Uk'37) for paleotemperature estimation in cold polar waters. Geochimica et Cosmochimica Acta 57, 1883-1889.

Surge, D.M., Lohmann, K.C., Goodfriend, G.A., 2003. Reconstructing estuarine conditions: oyster shells as recorders of environmental change, Southwest Florida. Estuarine, Coastal and Shelf Science 57, 737-756.

Surge, D., Barrett, J.H., 2012. Marine climatic seasonality during medieval times (10th to 12th centuries) based on isotopic records in Viking Age shells from Orkney, Scotland. Palaeogeography, Palaeoclimatology, Palaeoecology 350-352, 236-246.

Surge, D., Wang, T., Gutiérrez-Zugasti, I., Kelley, P.H., 2013. Isotope sclerochronology and season of annual growth line formation in limpet shells (*Patella vulgata*) from cold- and warm-temperate zones in the eastern North Atlantic. Palaios 28, 386-393.

Vanhaeren, M., d'Errico, F., 2006. Aurignacian ethno-linguistic geography of Europe revealed by personal ornaments. Journal of Archaeological Science 33, 1105-1128.

Wanamaker, A.D., Kreutz, K.J., Borns, H.W., Introne, D.S., Feindel, S., Barber, B.J.C.Q., 2006. An aquaculture-based method for calibrated bivalve isotope paleothermometry. Geochemistry, Geophysics, Geosystems 7, Q09011, doi:09010.01029/02005GC001189.

Wang, T., Surge, D., Mithen, S., 2012. Seasonal temperature variability of the Neoglacial (3300–2500 BP) and Roman Warm Period (2500–1600 BP) reconstructed from oxygen isotope ratios of limpet shells (*Patella vulgata*), Northwest Scotland. Palaeogeography, Palaeoclimatology, Palaeoecology 317–318, 104-113.

Figure captions

Fig. 1: Location of the study area in northern Iberia showing the location of shell and water collection zones (Langre, Somo, Astillero, La Cavada), the station where instrumental temperatures were obtained (El Bocal) and the main city in the area (Santander).

Fig. 2: Sampling strategies in *P. vulgata*: A) Inner part of a limpet shell showing the different layers of the shell and the sampling path followed to mill shell edge samples (dashed line); B) whole limpet shell showing position of cut along the growth axis; C) cross section of a limpet shell; D) Portion of a cross section displaying the position of calcite microstructures sampled in our study. Micromilling was performed following sampling paths along the growth lines and increments (dashed lines); E) Portion of a cross section stained with Mutvei´s solution displaying major and minor growth lines. DOG: direction of growth.

Fig. 3: Instrumental seawater temperatures obtained at El Bocal station (black circles) in 2011–2012 and mean monthly precipitation during the period 2011–2012 (black squares) in the study area (Source: Aemet, Spanish National Meteorology Agency).

Fig. 4: Oxygen isotope values of the seawater ($\delta^{18}O_{water}$) in different locations of the study area: Langre on the open coast (grey triangles), Somo in the estuary (grey circles), Astillero also in the estuary (black circles), and the river Miera at La Cavada (black squares). Significant differences can be observed between locations.

Fig. 5: Oxygen isotope values ($\delta^{18}O_{shell}$) from shell edge samples (six samples per collection event). Results show a clear sinusoidal pattern related to seasonal variations.

Fig. 6: A) Mean $\delta^{18}O_{shell}$ values from shell edge samples compared with predicted $\delta^{18}O_{shell}$ values calculated using instrumental seawater temperature (T_{meas}), $\delta^{18}O_{water}$, and

Eq. (1) and (2). Error bars were calculated using 1σ SD of the six samples measured per collection event. Results show a sinusoidal pattern related to seasonal variations in temperature and strong correlation between variables, suggesting that shells grew in isotopic equilibrium with the surrounding environment.

Fig. 7: Oxygen isotope values ($\delta^{18}O_{shell}$) from the four shells sampled sequentially (LAN25, LAN29, LAN43, LAN45). As with shell edge samples, results show a clear sinusoidal pattern related to seasonal variations.

Fig. 8: Calendar aligned shell oxygen isotope values ($\delta^{18}O_{shell}$) of shells sampled sequentially (LAN25, LAN29, LAN43, LAN45). Time calibration was performed using predicted $\delta^{18}O_{shell}$ values calculated from instrumental temperatures (T_{meas}) using the $\delta^{18}O_{water}$ and Eq. (1) and (2). Grey bars show periods of growth cessation, which mainly occurred in summer and winter (blue and orange lines). Lunar daily increment widths (LDIW) were measured for periods of growth.

Fig. 9: Mean reconstructed seawater temperature ($T_{\delta 18O}$) (black circles) using $\delta^{18}O_{shell}$, $\delta^{18}O_{water}$, and Eq. (1) and (2) compared with instrumental seawater temperature (T_{meas}) (grey diamonds). Error bars were calculated using 1σ SD of the six samples measured per collection event plus the replication precision error of the mass spectrometer. Both variables are highly correlated. Instrumental temperatures recorded at the time of collection are in the range of the standard deviation of calculated temperatures, except for the samples collected on the 5th August 2012 and 24th December 2011.

Fig. 10: Calendar aligned reconstructed temperature record ($T_{\delta 18O}$). Time calibration was the same as for the $\delta^{18}O_{shell}$. Grey bars show periods of growth cessation, which mainly occurred in summer and winter (blue and orange lines). Reconstructed temperatures (black circles) are mostly in agreement with instrumental temperatures (grey line). Deviations of reconstructed temperatures from instrumental temperatures were only identified in summer 2009 and summer/autumn 2010 of LAN25.

Fig. 11: Growth of shell LAN25 corresponding to ~12 weeks, between 26th October 2011 and 23rd January 2012. A) During that time interval, the area experienced six spring tide cycles (full moon open circles, new moon filled circle) and six neap tide cycles (circles open right=first quarter; open left=last quarter). The area was dominated by semidiurnal tidal cycles. B) Instrumental temperatures (T_{meas}) and reconstructed temperatures ($T_{\delta 18O}$) for the time period represented in that portion of growth. C) Cross section stained with Mutvei's solution showing fortnightly lines (white circles), coincident with spring tides. D) Detailed view of growth increments (circalunidian) limited by growth lines (circatidal). Lunidian growth increments are subdivided into two semilunidian increments by either a prominent or a faint line (marked as dashed lines). This pattern is typical of intertidal organisms and confirms that growth patterns are regulated by the tides. E) Microgrowth increments and lines formed over the course of one lunar cycle. Prominent growth lines and narrower increments were identified during full and new moon (spring tides), and thinner growth lines and strongly marked increments were formed during the first and last quarter of the moon (neap tides).

Table captions

Table 1: Seasonal oxygen isotope values of the seawater ($\delta^{18}O_{water}$) and salinity (S_{meas}) recorded at the location of shell collection (Langre) and other nearby environments: Somo (estuary), Astillero (estuary) and La Cavada (river).

Table 2: Offset recorded between measured and predicted $\delta^{18}O_{shell}$ using data on mean annual and seasonal $\delta^{18}O_{water}$ and instrumental temperatures at the time of shell collection, and four and six days before the shell collection.

Table 3: Size, shore zonation and oxygen isotope values ($\delta^{18}O_{shell}$) from shells used in the study (maximum, minimum and range), and number of annual cycles recorded in each shell.

Table 4: Difference between instrumental temperatures (T_{meas}) and reconstructed temperatures ($T_{\delta 18O}$) from shell edge samples.

Table 5: Instrumental temperatures (T_{meas}) and mean, maximum, minimum and range of reconstructed temperatures ($T_{\delta 18O}$) from shell edge samples (using the six samples per collection event, and all values) and shells sampled sequentially.

Table 6: Summary of growth patterns from shells sampled sequentially.

Table 7: Differences in reconstructed temperatures ($T_{\delta 18O}$) using different $\delta^{18}O_{water}$ values: monthly, mean annual, and maximum and minimum annual.

Figure 1
Click here to download high resolution image

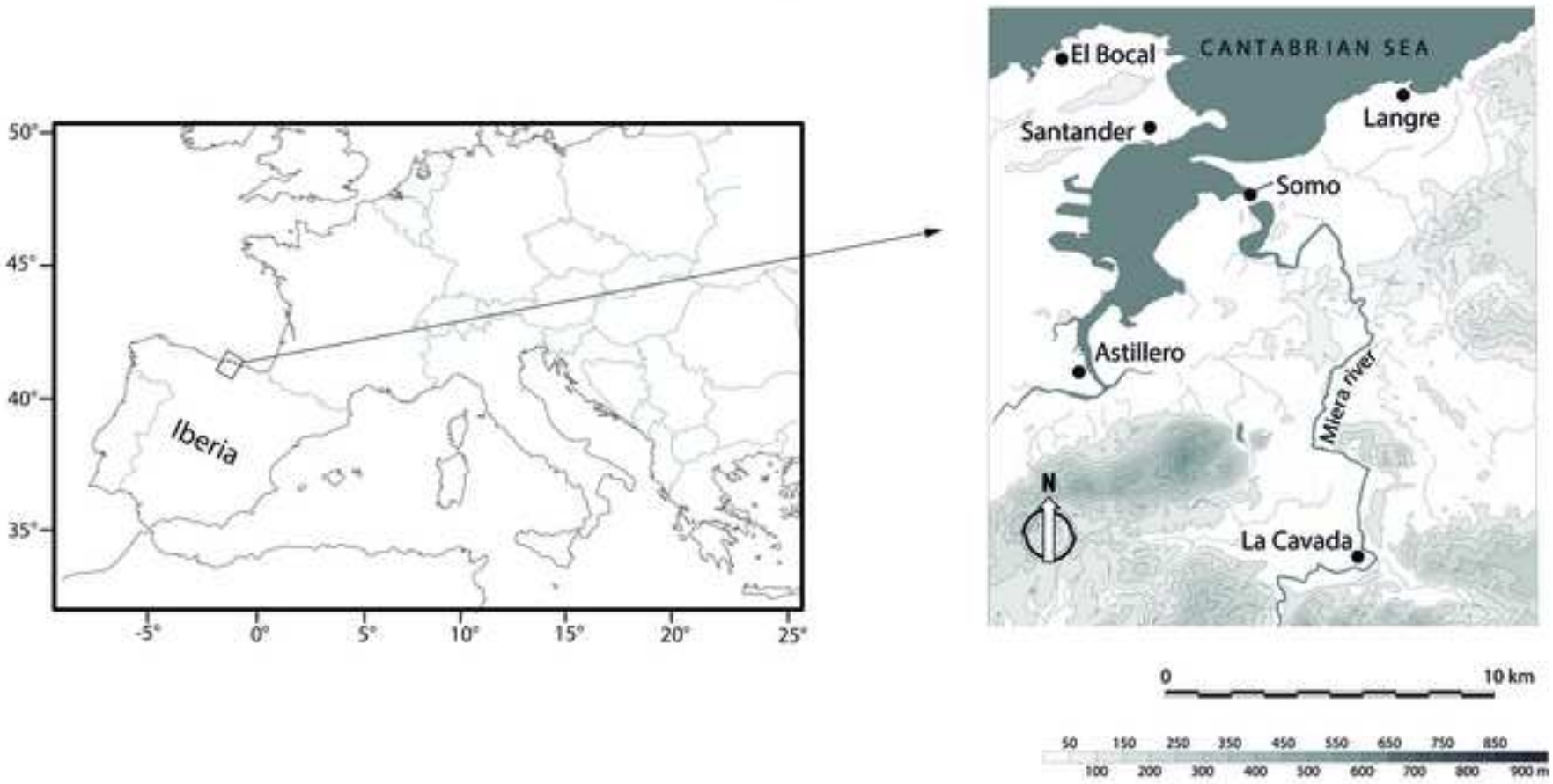

Figure 2
Click here to download high resolution image

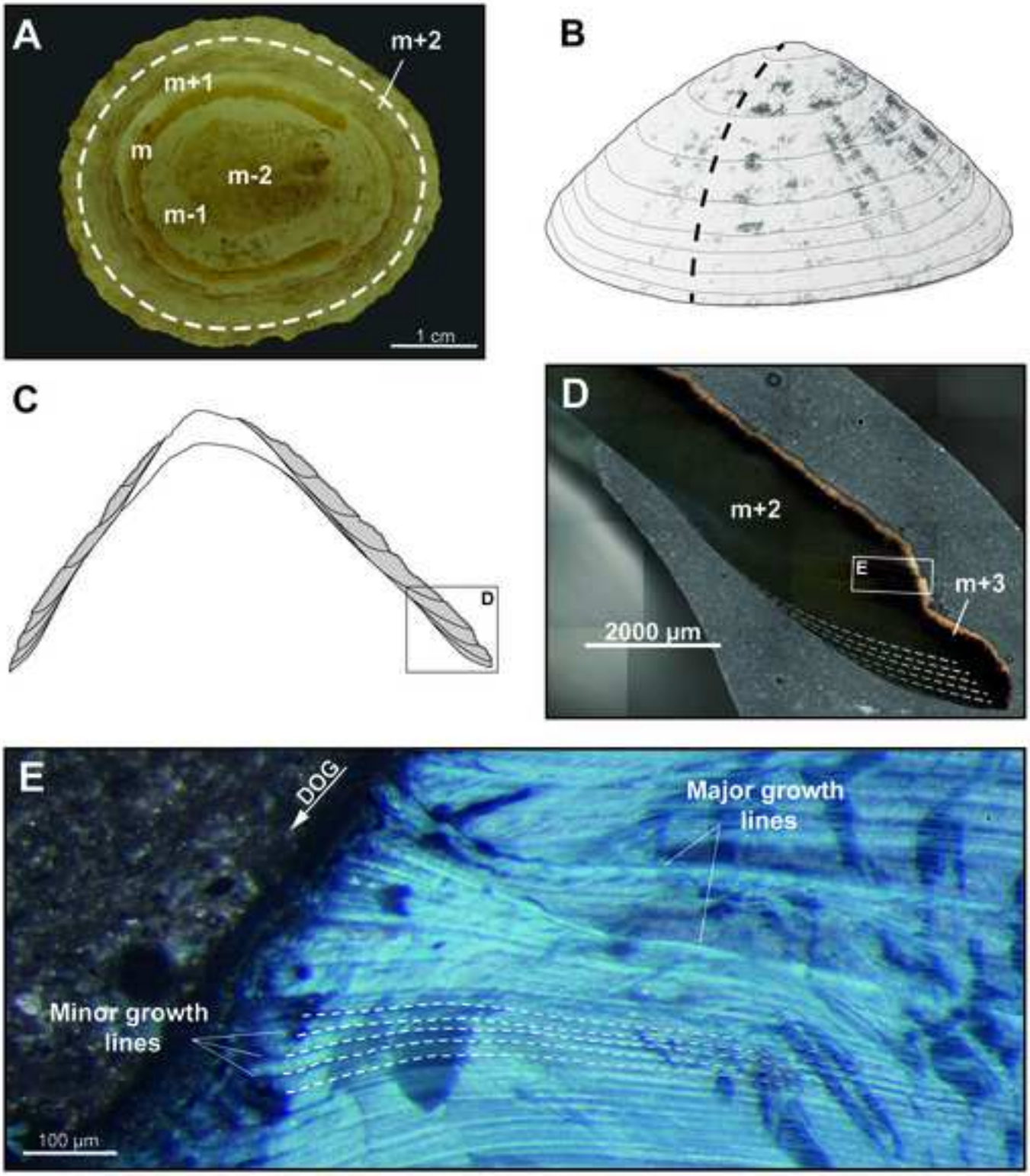

Figure 3
Click here to download high resolution image

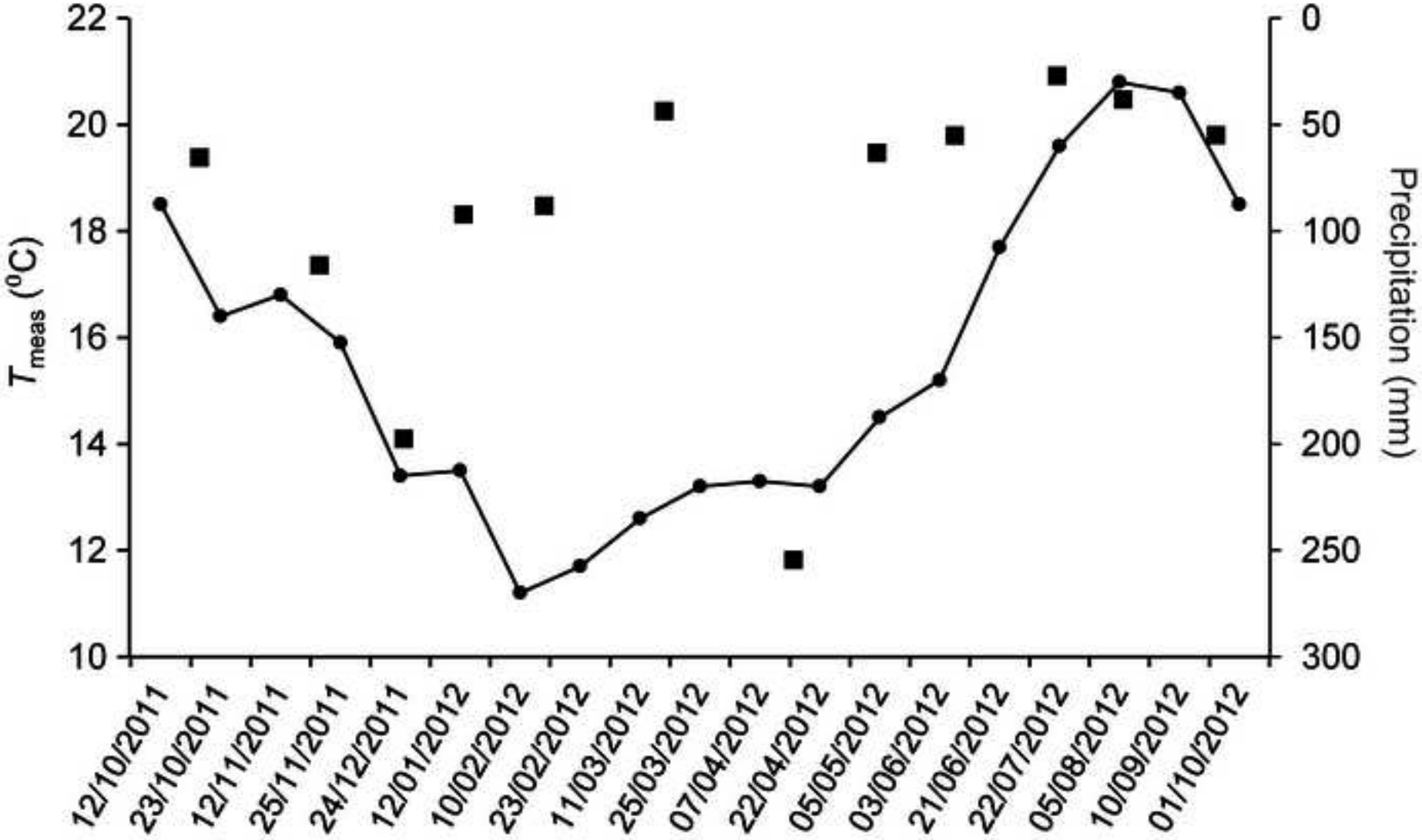

Figure 4
Click here to download high resolution image

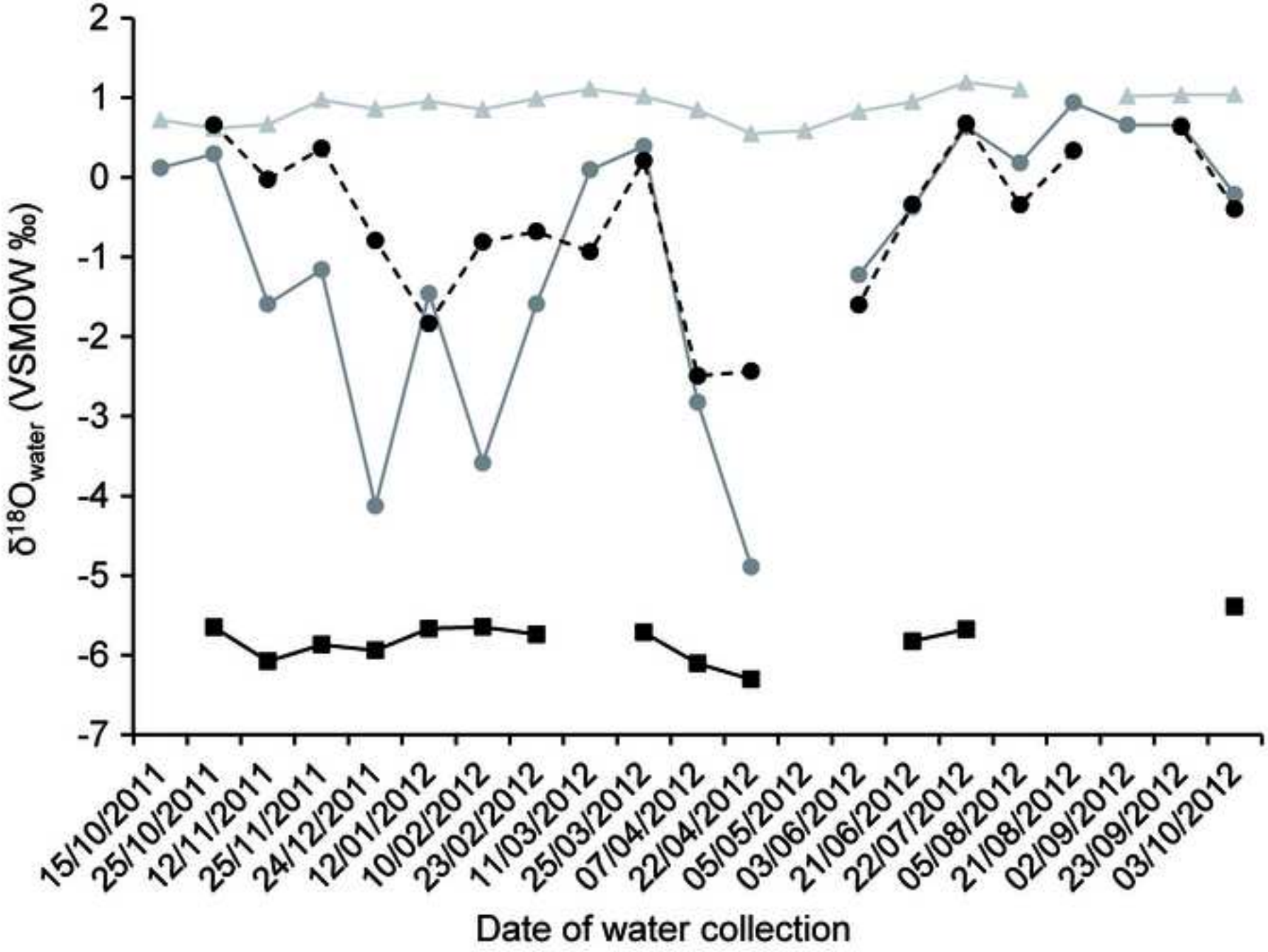

Figure 5
Click here to download high resolution image

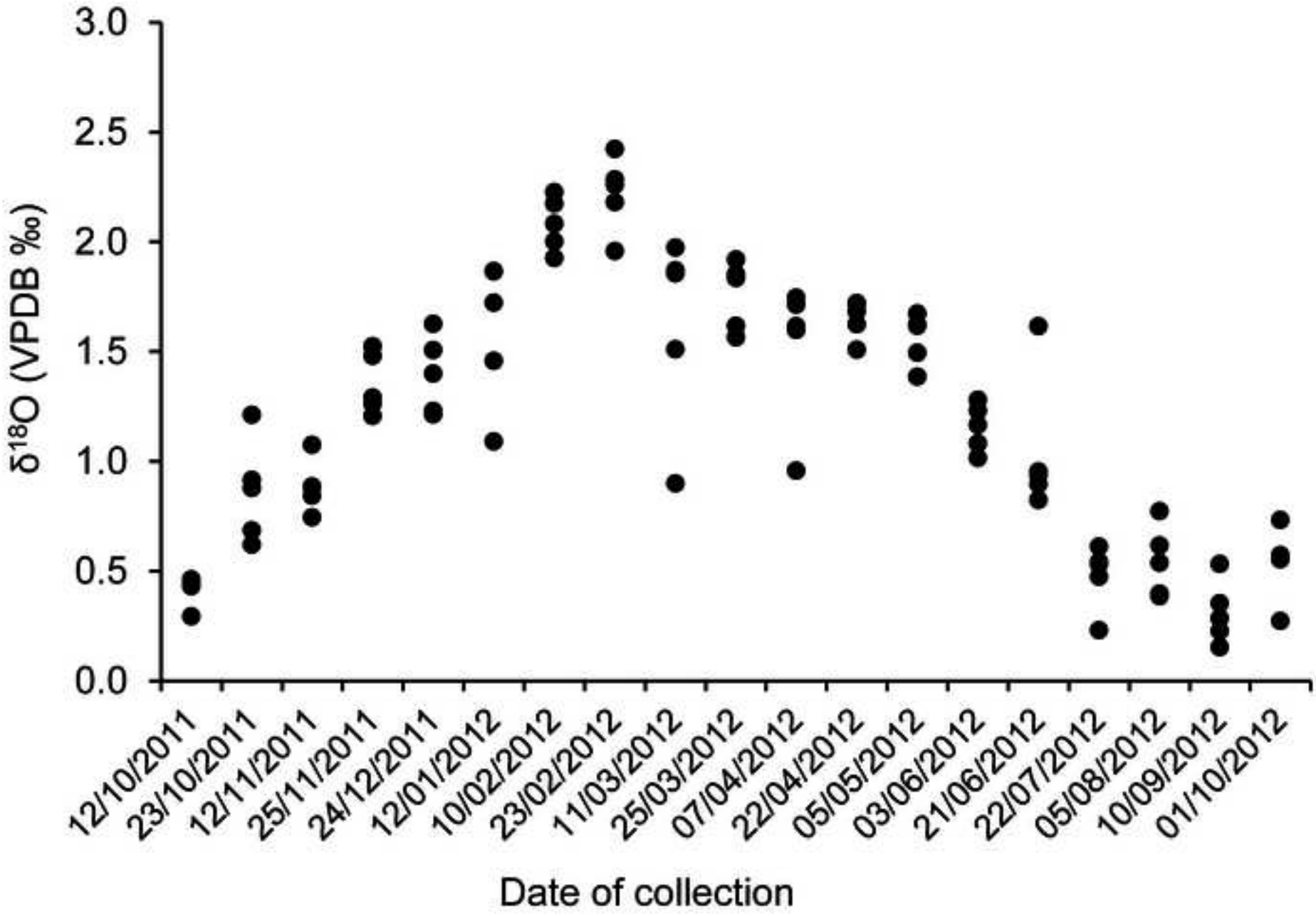

Figure 6
Click here to download high resolution image

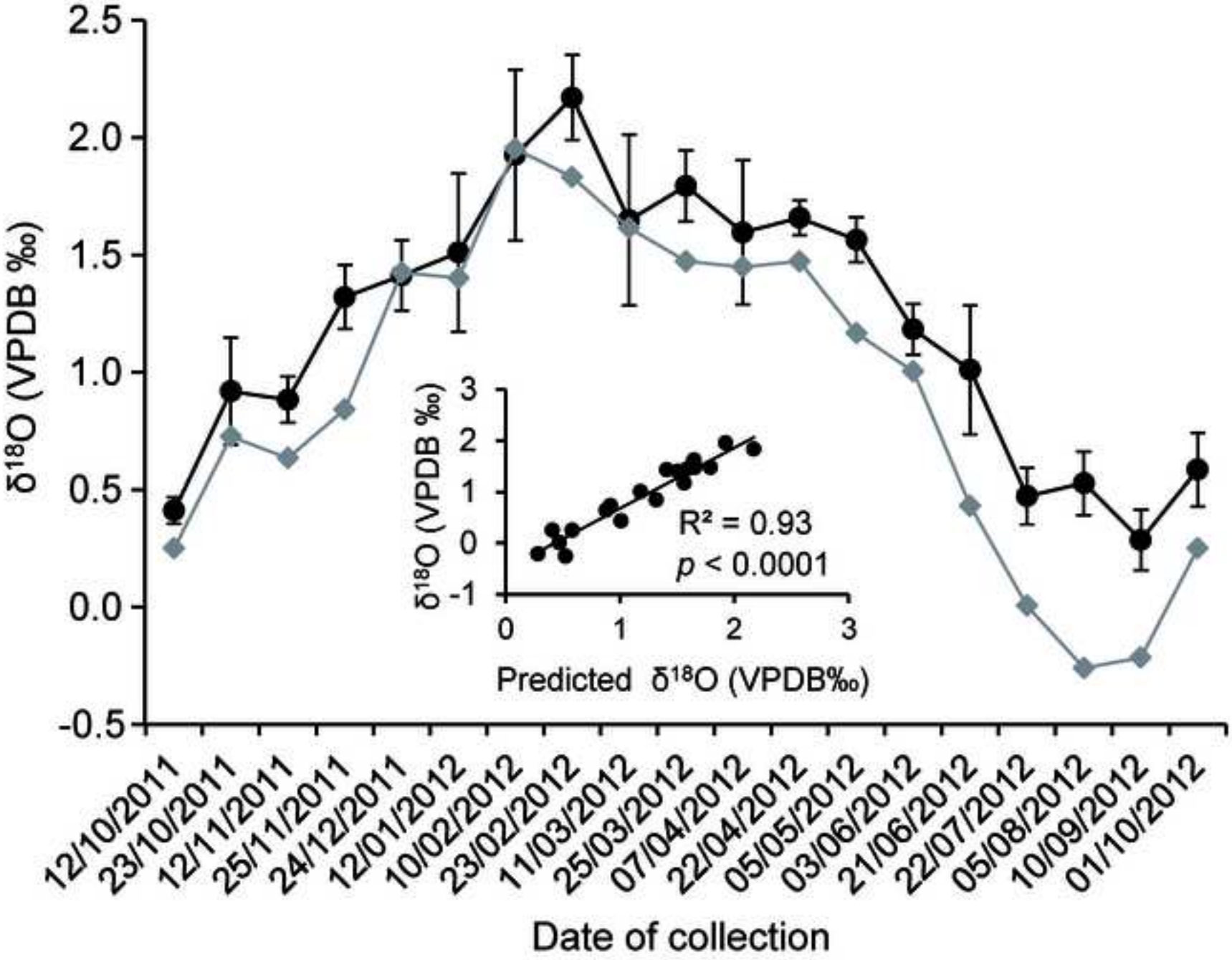

Figure 7
Click here to download high resolution image

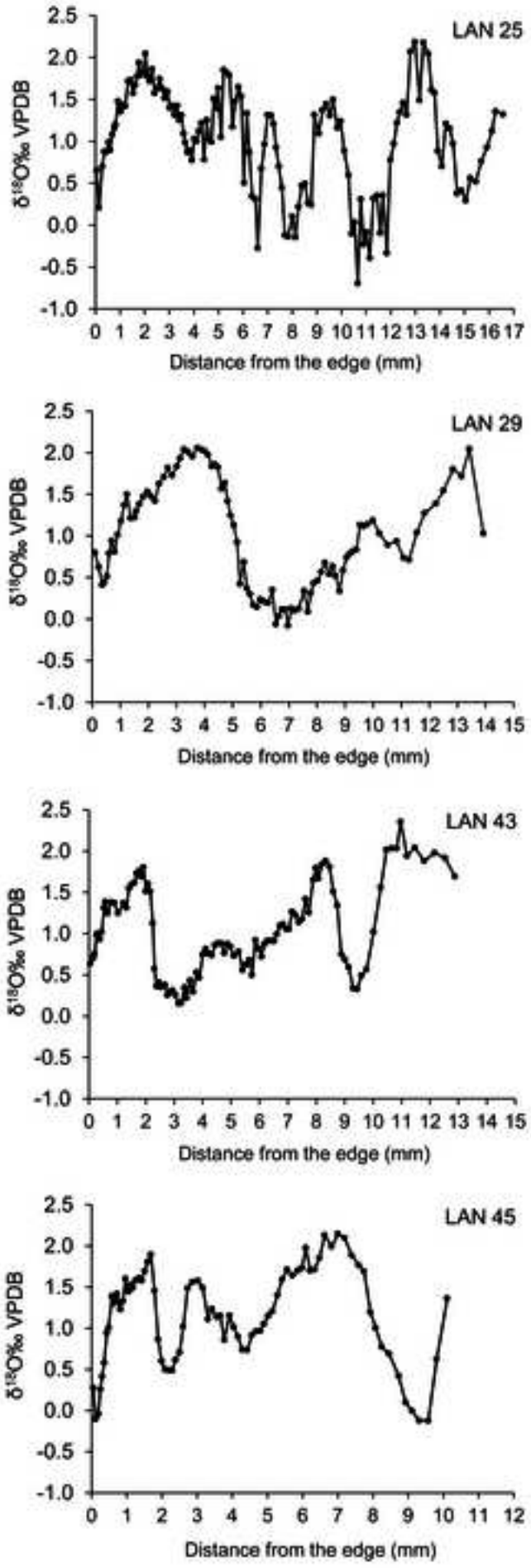

Figure 8

Click here to download high resolution image

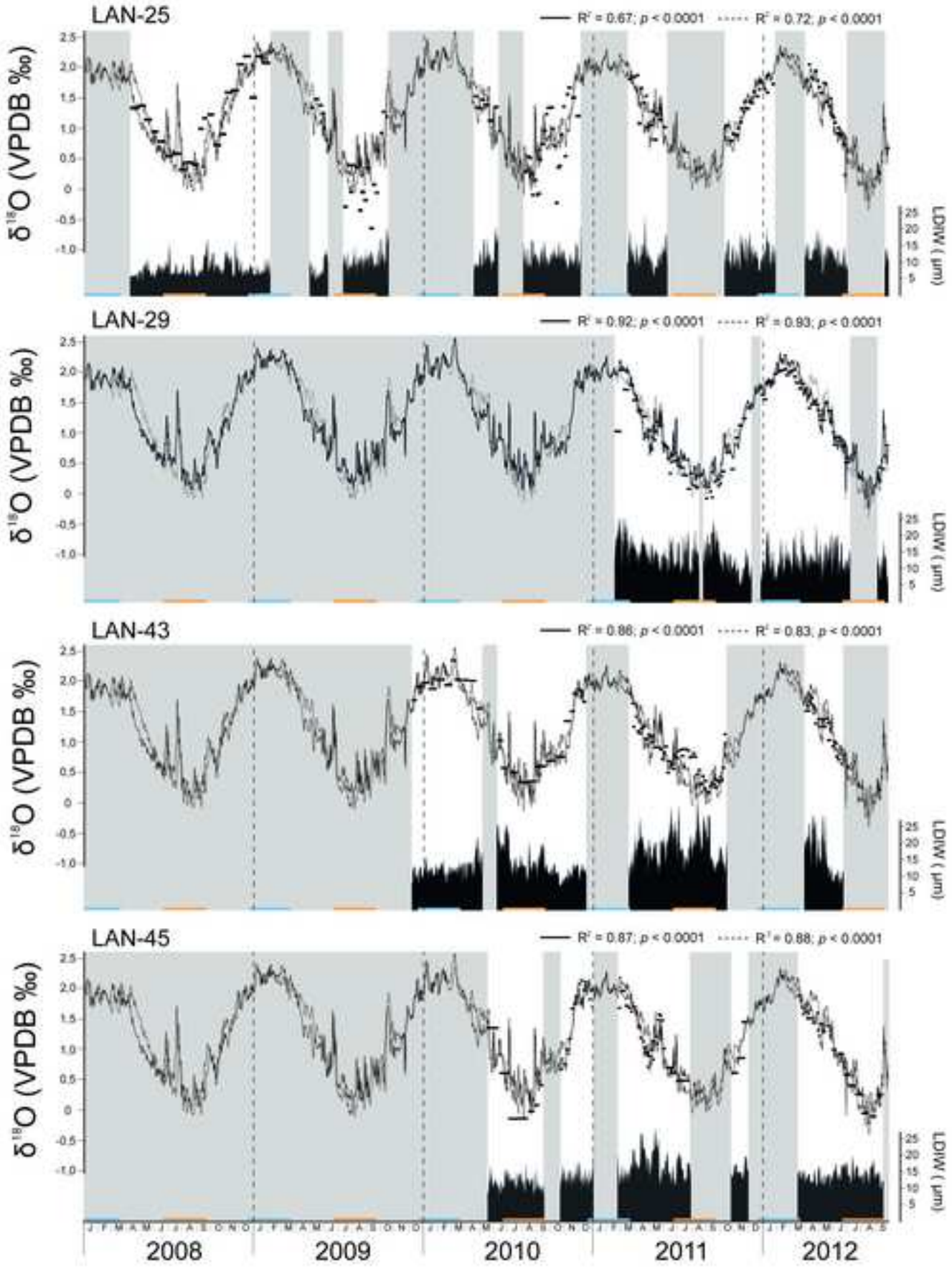

Figure 9
Click here to download high resolution image

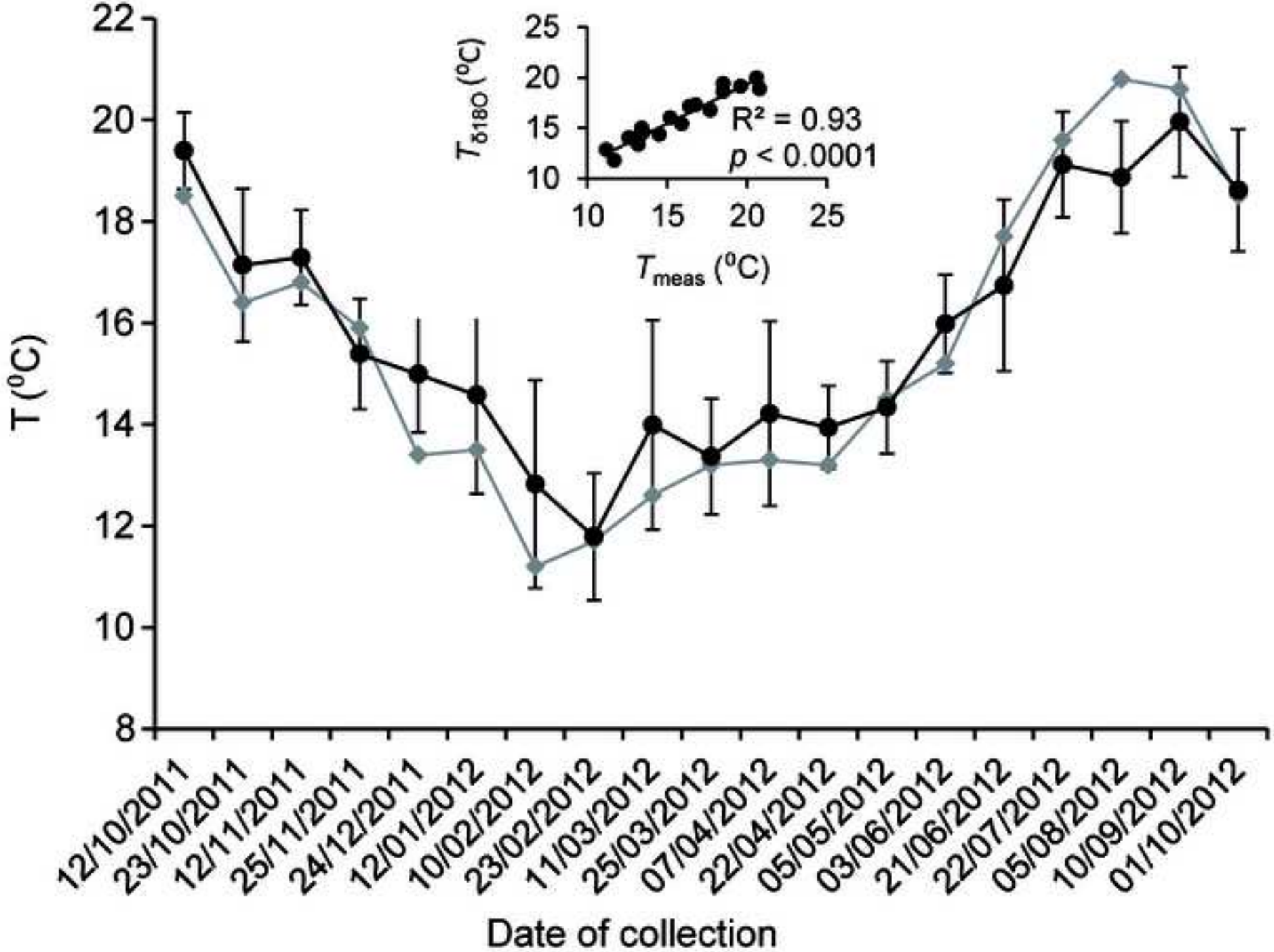

Figure 10
Click here to download high resolution image

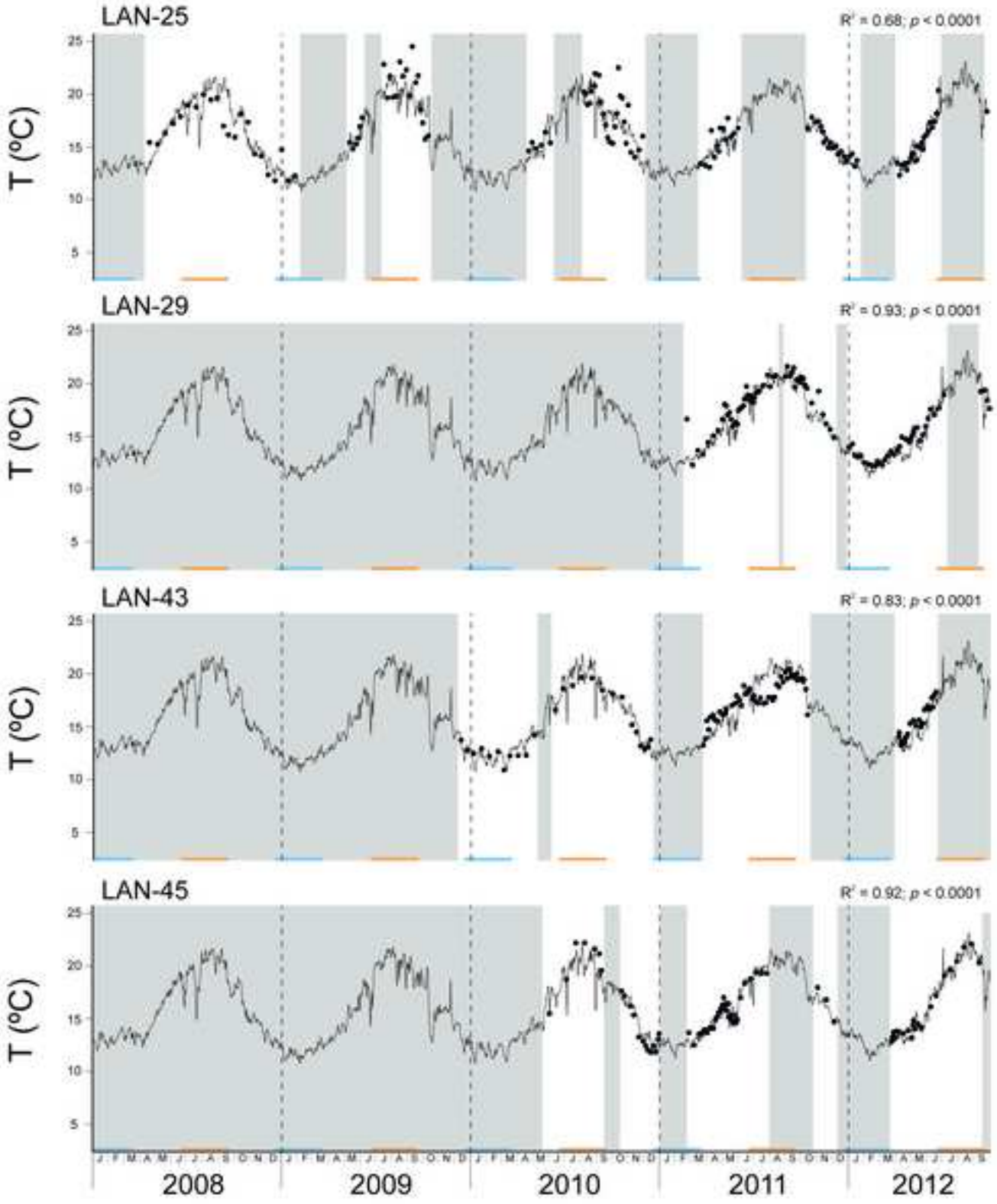

Figure 11

Click here to download high resolution image

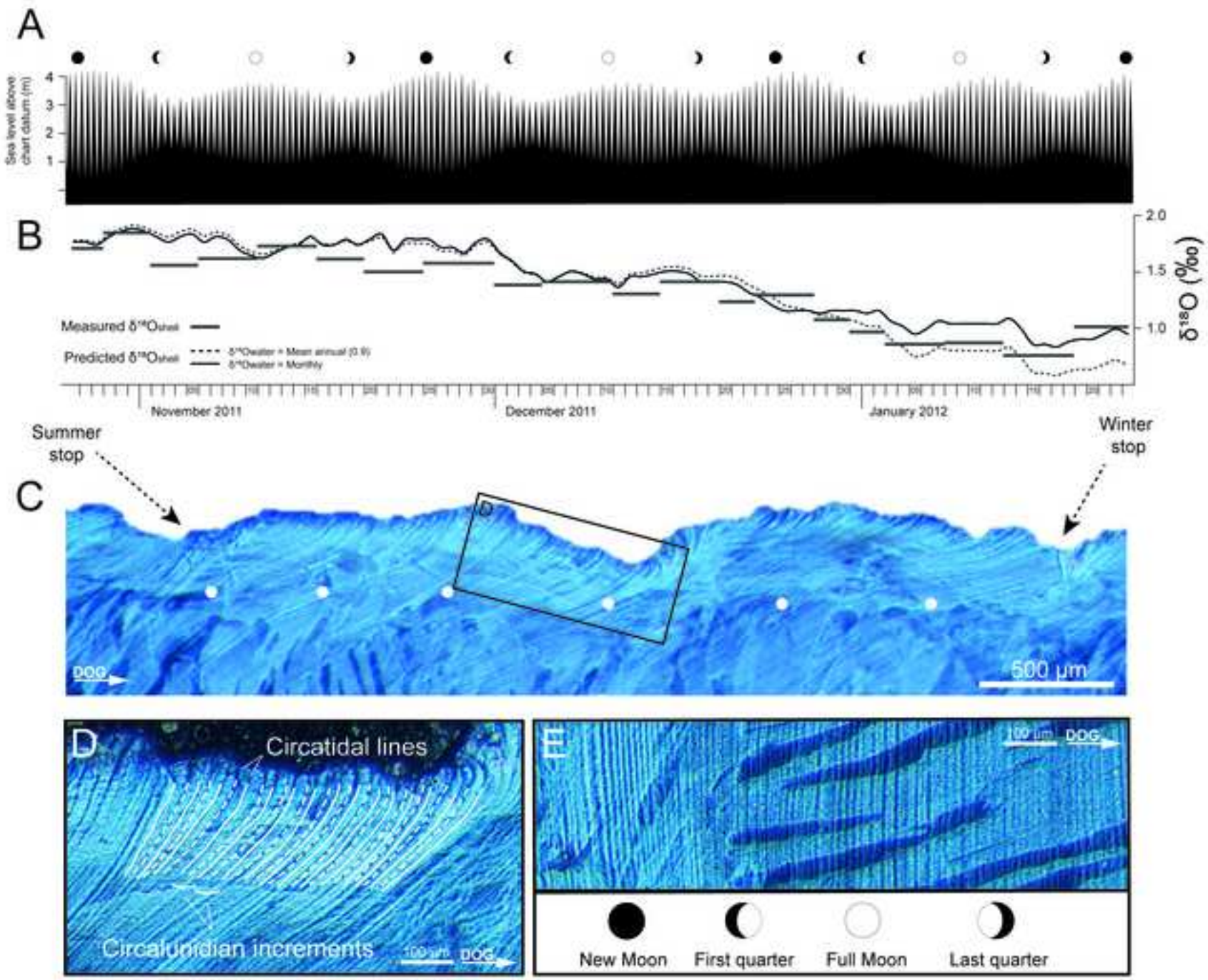

Table 1

Collection date	Langre		Somo		Astillero		La Cavada	
	$\delta^{18}O$‰ VSMOW	S_{meas} (PSU)	$\delta^{18}O$‰ VSMOW	S_{meas} (PSU)	$\delta^{18}O$‰ VSMOW	S_{meas} (PSU)	$\delta^{18}O$‰ VSMOW	S_{meas} (PSU)
10/15/2011	0.72	36.2	0.12	31.9				
10/25/2011	0.62	35.6	0.29	34	0.66	38.7	-5.65	<0.1
11/12/2011	0.67	35.3	-1.59	22.9	-0.03	30.8	-6.08	<0.1
11/25/2011	0.97	35.8	-1.16	24.6	0.36	33	-5.87	<0.1
12/24/2011	0.86	35.4	-4.12	8.3	-0.79	37.6	-5.94	<0.1
1/12/2012	0.95	35.9	-1.46	22.2	-1.83	19.9	-5.67	<0.1
2/10/2012	0.85	35	-3.58	10.6	-0.81	26.9	-5.65	<0.1
2/23/2012	0.99	35.6	-1.59	21.3	-0.68	26.4	-5.74	<0.1
3/11/2012	1.11	35.5	0.09	30	-0.93	23.6		
3/25/2012	1.02	35.5	0.39	31.8	0.21	31.1	-5.71	<0.1
4/7/2012	0.85	35.5	-2.82	16.7	-2.49	26.5	-6.10	<0.1
4/22/2012	0.55	34	-4.89	5.3	-2.44	17.6	-6.30	<0.1
5/5/2012	0.59	34.1						
6/3/2012	0.83	36.9	-1.22	25.5	-1.60	22.4		
6/21/2012	0.95	35.6	-0.38	27.7	-0.34	32.2	-5.82	<0.1
7/22/2012	1.19	35.7	0.64	25.4	0.68	33.8	-5.67	<0.1
8/5/2012	1.10	35.7	0.18	31	-0.34	27.6		
8/21/2012			0.94	35.5	0.34	35.6		
9/2/2012	1.02	35.9	0.66	35.8				
9/23/2012	1.04	37.1	0.66	32.5	0.63	32.3		
10/3/2012	1.04	36	-0.22	29.9	-0.40	26.7	-5.39	<0.1
Mean	0.90	35.6	-0.95	25.1	-0.55	29.0	-5.82	<0.1
Max	1.19	37.1	0.94	35.8	0.68	38.7	-5.39	<0.1
Min	0.55	34	-4.89	5.3	-2.49	17.6	-6.30	<0.1
Range	0.64	3.1	5.83	30.5	3.17	21.1	0.91	<0.1

Table 2

	Annual $\delta^{18}O_{water}$			Seasonal $\delta^{18}O_{water}$		
Season	Collection date	4 days prior to shell collection	6 days prior to shell collection	Collection date	4 days prior to shell collection	6 days prior to shell collection
Summer	0.55	0.54	0.54	0.40	0.38	0.40
Spring	0.27	0.23	0.22	0.41	0.37	0.35
Winter	0.24	0.27	0.28	0.19	0.23	0.24
Autumn	0.35	0.40	0.39	0.40	0.46	0.46
Annual	0.34	0.35	0.35	0.36	0.35	0.35

Table 3

Sample	Size (mm)	Shore Zonation	Max	Min	Range	Annual $\delta^{18}O$ cycles
LAN25	45.6	High	2.18	-0.70	2.88	4.5
LAN29	37.6	High	2.06	-0.08	2.14	1.5
LAN43	42	Low	2.37	0.17	2.20	2.5
LAN45	37.5	Low	2.14	-0.12	2.27	3.0

Table 4

Collection date	T_{meas} (ºC)	$T_{\delta 18O}$ (ºC)	SD	Difference T_{meas} - $T_{\delta 18O}$ (ºC)
10/1/2012	18.5	18.6	0.7	-0.1
9/10/2012	20.6	20.0	0.6	0.6
8/5/2012	20.8	18.9	0.6	1.9
7/22/2012	19.6	19.1	0.5	0.5
6/21/2012	17.7	16.7	1.2	1.0
6/3/2012	15.2	16.0	0.5	-0.8
5/5/2012	14.5	14.3	0.4	0.2
4/22/2012	13.2	13.9	0.3	-0.7
4/7/2012	13.3	14.2	1.3	-0.9
3/25/2012	13.2	13.4	0.6	-0.2
3/11/2012	12.6	14.0	1.6	-1.4
2/23/2012	11.7	11.8	0.7	-0.1
2/10/2012	11.2	12.8	1.5	-1.6
1/12/2012	13.5	14.6	1.4	-1.1
12/24/2011	13.4	15.0	0.6	-1.6
11/25/2011	15.9	15.4	0.6	0.5
11/12/2011	16.8	17.3	0.4	-0.5
10/23/2011	16.4	17.1	1.0	-0.7
10/12/2011	18.5	19.4	0.3	-0.9
Mean	15.6	15.9	0.8	-0.3
Max	20.8	20.0	1.6	1.9
Min	11.2	11.8	0.3	-1.6
Range	9.6	8.2	1.3	3.5

Table 5

	T_{meas} (Collection events)	$T_{\delta18O}$ (Shell edge - Collection events)	$T_{\delta18O}$ (Shell edge - All values)	T_{meas} (2007-2012)	$T_{\delta18O}$ (LAN25)	$T_{\delta18O}$ (LAN29)	$T_{\delta18O}$ (LAN43)	$T_{\delta18O}$ (LAN45)
Mean	15.6	15.9	15.9	15.8	16.4	16.7	16.2	15.8
SD	2.9	2.4	2.5	3.1	3.0	3.0	2.5	2.7
Max	20.8	20.0	20.6	23.1	24.9	22.0	20.9	22.2
Min	11.2	11.8	10.7	10.8	11.3	12.2	10.9	11.9
Range	9.6	8.1	9.8	12.3	13.6	9.8	10.0	10.3

Table 6

Sample ID	Shell growth (days)	Shell lifetime (days)	% of days growing	Averaged lunar daily increment width (μm)	Number of days per isotopic sample	
					Max	Min
LAN25	875	1550	56	10.2	13.6	4.2
LAN29	461	585	79	13.1	5.5	4.8
LAN43	602	1017	59	12.7	19	3
LAN45	455	860	53	13.2	18	4.3

Table 7

Collection date	T_{meas}	$T_{\delta 18O}$ (monthly $\delta^{18}O_{water}$)	$T_{\delta 18O}$ (mean annual $\delta^{18}O_{water}$)	Difference in $T_{\delta 18O}$ using mean annual and collection event $\delta^{18}O_{water}$	$T_{\delta 18O}$ (maximum $\delta^{18}O_{water}$)	$T_{\delta 18O}$ (minimum $\delta^{18}O_{water}$)	Difference in $T_{\delta 18}O$ using maximum and minimum $\delta^{18}O_{water}$
10/1/2012	18.5	19.2	18.6	-0.6	19.9	17.1	2.9
9/10/2012	20.6	20.5	20.0	-0.5	21.3	18.4	2.9
8/5/2012	20.8	19.8	18.9	-0.9	20.2	17.3	2.9
7/22/2012	19.6	20.4	19.1	-1.3	20.4	17.6	2.9
6/21/2012	17.7	17.0	16.7	-0.2	18.0	15.2	2.8
6/3/2012	15.2	15.7	16.0	0.3	17.3	14.5	2.8
5/5/2012	14.5	13.0	14.3	1.3	15.6	12.9	2.7
4/22/2012	13.2	12.5	13.9	1.5	15.2	12.5	2.7
4/7/2012	13.3	14.0	14.2	0.2	15.5	12.7	2.7
3/25/2012	13.2	13.9	13.4	-0.5	14.6	11.9	2.7
3/11/2012	12.6	14.9	14.0	-0.9	15.2	12.5	2.7
2/23/2012	11.7	12.2	11.8	-0.4	13.0	10.3	2.7
2/10/2012	11.2	12.6	12.8	0.2	14.0	11.4	2.7
1/12/2012	13.5	14.8	14.6	-0.2	15.8	13.1	2.7
12/24/2011	13.4	14.8	15.0	0.2	16.2	13.5	2.7
11/25/2011	15.9	15.7	15.4	-0.3	16.6	13.9	2.8
11/12/2011	16.8	16.3	17.3	1.0	18.6	15.8	2.8
10/23/2011	16.4	15.9	17.1	1.2	18.4	15.6	2.8
10/12/2011	18.5	18.6	19.4	0.8	20.7	17.8	2.9
Mean	15.6	15.9	15.9	0.0	17.2	14.4	2.8
Max	20.8	20.5	20.0	1.5	21.3	18.4	2.9
Min	11.2	12.2	11.8	-1.3	13.0	10.3	2.7
Range	9.6	8.3	8.2	2.8	8.3	8.1	0.2